Heliyon 9 (2023) e22402

Contents lists available at ScienceDirect

Heliyon

journal homepage: www.cell.com/heliyon

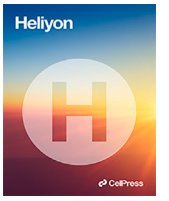

Research article

The type II exponentiated half logistic-odd Burr X-G power series class of distributions with applications

Neo Dingalo *, Broderick Oluyede, Fastel Chipepa

Botswana International University of Science and Technology P. Bag 16, Palapye, Botswana

ARTICLE INFO

MSC:
62E99
60E05

Keywords:
Odd Burr-X distribution
Goodness-of-fit statistics
Power series distribution
Simulation study

ABSTRACT

A new distribution, the type II exponentiated half logistic-odd Burr X-G power series (TII-EHL-OBX-GPS), is introduced in this study. This distribution combines the type II exponentiated half logistic-odd Burr X-G family of distributions with power series distributions. We discuss its mathematical characteristics, maximum likelihood estimates and simulation experiments, along with practical applications in the type II exponentiated half logistic-odd Burr X-log-logistic Poisson distribution.

1. Introduction

In the field of statistics, researchers continually seek distributions that can effectively capture the complexities of real-world data. The limitations of classical distributions have prompted the development of new, generalized classes of probability distributions.

In recent years, several generalizations have emerged, including the type II- exponentiated half logistic (EHL)-G family of distributions (FoD) [4], type II-EHL-Gompertz-G FoD [23], type II -EHL-Gompertz-Topp-Leone-G FoD [30], type II-EHL-Topp-Leone Marshall-Olkin-G FoD [25], type II half logistic distribution [37], type II half logistic exponentiated-G FoD [7], new type II half logistic-G FoD [5], type II general inverse exponential distribution [16], Burr X-exponentiated Weibull distribution [18], Marshall-Olkin Burr-X-G FoD [17], beta-Burr-X FoD [22], type I Burr-X-G FoD [3], Weibull-Burr-X-G FoD [15] and beta Kumaraswamy-Burr-X-G FoD [19]. These distributions have expanded the toolbox of statistical modeling, allowing researchers to address a wider range of data characteristics.

Simultaneously, researchers have explored power series (PS) distributions as alternative for data fitting. They include the type II-EHL-Topp-Leone-G PS class of distributions (CoD) [24], EHL- Topp-Leone-G PS CoD introduced [10], exponentiated-G PS CoD introduced by [29], odd power generalised Weibull-Weibull Poisson CoD [31], odd Lindely-G PS CoD [8], exponentiated half-logistic power generalized Weibull-G FoD [27], exponentiated power Lindely Poisson distribution [33], Ristic Balakrishnan Lindely Poisson distribution [14], odd Weibull-Topp-Leone-G PS CoD [26], Topp-Leone-G PS CoD [21], Burr XII Weibull Logarithmic distribution [28], generalized Burr XII PS CoD [13], Lindely Burr XII PS CoD [20], T-R Y PS CoD [32], inverse Lindley PS CoD [35] and exponentiated extended Weibull PS CoD [38], to mention just a few.

To enhance the flexibility of the type II-exponentiated half logistic-odd Burr X-G power series (TII-EHL-OBX-GPS) CoD, we introduce an additional parameter. This added parameter significantly impacts both scale and shape parameters. We illustrate these effects

* Corresponding author.
E-mail address: neo.dingalo@studentmail.biust.ac.bw (N. Dingalo).

https://doi.org/10.1016/j.heliyon.2023.e22402
Received 12 May 2023; Received in revised form 1 November 2023; Accepted 10 November 2023

Available online 17 November 2023

by examining probability density function (pdf) and hazard rate function (hrf) plots, as well as skewness (SK) and kurtosis (KS) plots, and by applying it to real-world data examples. The TII-EHL-OBX-GPS CoD, can capture a diverse range of density functions shapes such as negative skewness, positive skewness, symmetric, J-shaped, and reverse J-shaped distributions. Incorporating monotonic and non-monotonic patterns into the hrf of the TII-EHL-OBX-GPS CoD offers several advantages, including increased flexibility, improved data fitting, the capability to handle complex data characteristics, improved reliability analysis, and wider applicability.

The arrangement of the study proceeds as follows: Section 2 presents the development and mathematical properties of the TII-EHL-OBX-GPS CoD. In Section 3, we provide visual representations of the pdf and hrf, as well as 3D plots displaying skewness (SK) and kurtosis (KS) for the special classes of the TII-EHL-OBX-GPS CoD. Sections 4 and 5 discuss the maximum likelihood estimation (MLE) method and simulation experiments, respectively. Section 6 contains some applications from different fields. Section 7 gives the conclusion and summary.

2. The model

Here, we develop the TII-EHL-OBX-GPS CoD by first considering a series of N random variables that are both independent and identically distributed, say Z_j, j = 1,..., N, from the TII-EHL-OBX-G FoD. The cumulative density function (cdf) of Z is

$$F_{TII-EHL-OBX-G}(z;\beta,q,\underline{\kappa}) = 1 - \left[\frac{1-\mathrm{H}(z;\beta,\underline{\kappa})}{1+\mathrm{H}(z;\beta,\underline{\kappa})}\right]^q,$$

and the pdf is

$$\begin{aligned} f_{TII-EHL-OBX-G}(z;\beta,q,\underline{\kappa}) &= 4q\beta\left(1-\mathrm{H}(z;\beta,\underline{\kappa})\right)^{q-1}\left(1+\mathrm{H}(z;\beta,\underline{\kappa})\right)^{-(q+1)} \\ &\times\left(1-\exp\left(-\left(\frac{G(z;\underline{\kappa})}{1-G(z;\underline{\kappa})}\right)^2\right)\right)^{\beta-1} \\ &\times\exp\left(-\left(\frac{G(z;\underline{\kappa})}{1-G(z;\underline{\kappa})}\right)^2\right)\left(1-G(z;\underline{\kappa})\right)^{-3} G(z;\underline{\kappa})g(z;\underline{\kappa}), \end{aligned}$$

respectively, in which $\mathrm{H}(z;\beta,\underline{\kappa}) = \left(1-\exp\left(-\left(\frac{G(z;\underline{\kappa})}{1-G(z;\underline{\kappa})}\right)^2\right)\right)^{\beta}$ for $z,q,\beta>0$, and parent parameter vector $\underline{\kappa}$. The survival function (sf) is

$$\begin{aligned} S_{TII-EHL-OBX-G}(z;q,\beta,\underline{\kappa}) &= 1 - F_{TII-EHL-OBX-G}(z;\beta,q,\underline{\kappa}) \\ &= \left[\frac{1-\mathrm{H}(z;\beta,\underline{\kappa})}{1+\mathrm{H}(z;\beta,\underline{\kappa})}\right]^q. \end{aligned}$$

We combine the TII-EHL-OBX-G FoD with the PS CoD. Assume N is a zero truncated discrete random variable having a PS distribution defined as

$$P(N=n) = \frac{a_n \upsilon^n}{C(\upsilon)}, n = 1,2,3,...,$$

$C(\upsilon) = \sum_{n=1}^{\infty} a_n \upsilon^n$ is finite, $\upsilon>0$ and $\{a_n\}_{n\geq 1}$ a sequence of non-negative integers. If we consider $Z_{(1)} = \min(Z_1, Z_2, ..., Z_N)$, we obtain the cdf of $Z_{(1)}|N=n$ as

$$F_{Z_{(1)}|N=n}(z;q,\beta,\underline{\kappa}) = 1 - \left(\left[\frac{1-\mathrm{H}(z;\beta,\underline{\kappa})}{1+\mathrm{H}(z;\beta,\underline{\kappa})}\right]^q\right)^n,$$

for $q,\beta>0$ and parameter vector $\underline{\kappa}$.

The TII-EHL-OBX-GPS CoD is the marginal distribution of $Z_{(1)}$ with the cdf and pdf defined by

$$F_{Z_{(1)}}(z) = 1 - \frac{C(\upsilon S_{TII-EHL-OBX-G}(z;\beta,q,\underline{\kappa}))}{C(\upsilon)} \tag{1}$$

and

$$f_{Z_{(1)}}(z) = \frac{\upsilon g(z;\underline{\kappa})C'(\upsilon S_{TII-EHL-OBX-G}(z;\beta,q,\underline{\kappa}))}{C(\upsilon)},$$

where $S_{TII-EHL-OBX-G}(z;\beta,q,\underline{\kappa})$ is the sf of the TII-EHL-OBX-G FoD and $\underline{\kappa}$ is a parameter vector of the parent cdf $G(z;\underline{\kappa})$, with pdf $g(z;\underline{\kappa})$.

Using equation (1), the TII-EHL-OBX-GPS CoD has the cdf and pdf defined by

$$F_{TII-EHL-OBX-GPS}(z) = 1 - \frac{C\left(\upsilon\left[\frac{1-\mathrm{H}(z;\beta,\underline{\eta})}{1+\mathrm{H}(z;\beta,\underline{\eta})}\right]^q\right)}{C(\upsilon)}, \tag{2}$$

Table 1
Some Cases - TII-EHL-OBX-GPS Class of Distributions.

Some Cases	cdf
TII-EHL-OBX-G Poisson	$1-\frac{\exp\left(\upsilon\left(\left[\frac{1-\mathrm{H}(z;\beta,\underline{\kappa})}{1+\mathrm{H}(z;\beta,\underline{\kappa})}\right]^{q}\right)\right)-1}{\exp(\upsilon)-1}$
TII-EHL-OBX-G Geometric	$1-\frac{(1-\upsilon)\left[\frac{1-\mathrm{H}(z;\beta,\underline{\kappa})}{1+\mathrm{H}(z;\beta,\underline{\kappa})}\right]^{q}}{\left(1-\upsilon\left[\frac{1-\mathrm{H}(z;\beta,\underline{\kappa})}{1+\mathrm{H}(z;\beta,\underline{\kappa})}\right]^{q}\right)}$
TII-EHL-OBX-G Logarithmic	$1-\frac{\log\left(1-\upsilon\left[\frac{1-\mathrm{H}(z;\beta,\underline{\kappa})}{1+\mathrm{H}(z;\beta,\underline{\kappa})}\right]^{q}\right)}{\log(1-\upsilon)}$
TII-EHL-OBX-G Binomial	$1-\frac{\left(1+\upsilon\left[\frac{1-\mathrm{H}(z;\beta,\underline{\kappa})}{1+\mathrm{H}(z;\beta,\underline{\kappa})}\right]^{q}\right)^{m}-1}{(1+\upsilon)^{m}-1}$

and

$$
\begin{aligned}
f_{TII-EHL-OBX-GPS}(z) &= 4q\beta\upsilon\left(1-\mathrm{H}(z;\beta,\underline{\kappa})\right)^{q-1}\left(1+\mathrm{H}(z;\beta,\underline{\kappa})\right)^{-(q+1)} \\
&\times\left(1-\exp\left(-\left(\frac{G(z;\underline{\kappa})}{1-G(z;\underline{\kappa})}\right)^{2}\right)\right)^{\beta-1} \\
&\times\exp\left(-\left(\frac{G(z;\underline{\kappa})}{1-G(z;\underline{\kappa})}\right)^{2}\right)\left(1-G(z;\underline{\kappa})\right)^{-3}G(z;\underline{\kappa})g(z;\underline{\kappa}) \\
&\times\frac{C'\left(\upsilon\left[\frac{1-\mathrm{H}(z;\beta,\underline{\kappa})}{1+\mathrm{H}(z;\beta,\underline{\kappa})}\right]^{q}\right)}{C(\upsilon)},
\end{aligned}
\tag{3}
$$

respectively, for $z, q, \upsilon\ \beta > 0$, and parent parameter vector $\underline{\kappa}$.

We illustrate particular cases for the TII-EHL-OBX-GPS CoD in which the definition of $C(\upsilon)$ aligns with equation (2) in Table 1.

2.1. Some sub-classes

Some sub-classes of TII-EHL-OBX-GPS CoD are obtained by setting $\beta = 1$, $q = 1$, $q = \beta = 1$, $q = \beta = 1$ and $\upsilon \to 0^{+}$, $q = 1$ and $\upsilon \to 0^{+}$, to get the following sub-classes and sub-families of distributions with their cdf given as

$$
F(z;\upsilon,q,\underline{\kappa}) = 1-\frac{C\left(\upsilon\left[\frac{\exp\left(-\left(\frac{G(z;\underline{\kappa})}{1-G(z;\underline{\kappa})}\right)^{2}\right)}{1+\left(1-\exp\left(-\left(\frac{G(z;\underline{\kappa})}{1-G(z;\underline{\kappa})}\right)^{2}\right)\right)}\right]^{q}\right)}{C(\upsilon)},
$$

for $\upsilon, q > 0$ and parameter vector $\underline{\kappa}$,

$$
F(z;\beta,\upsilon,\underline{\kappa}) = 1-\frac{C\left(\upsilon\left[\frac{1-\mathrm{H}(z;\beta,\underline{\kappa})}{1+\mathrm{H}(z;\beta,\underline{\kappa})}\right]\right)}{C(\upsilon)},
$$

for $\upsilon, \beta > 0$ and baseline parameter vector $\underline{\kappa}$,

$$
F(z;\upsilon,\underline{\kappa}) = 1-\frac{C\left(\upsilon\left[\frac{\exp\left(-\left(\frac{G(z;\underline{\kappa})}{1-G(z;\underline{\kappa})}\right)^{2}\right)}{1+\left(1-\exp\left(-\left(\frac{G(z;\underline{\kappa})}{1-G(z;\underline{\kappa})}\right)^{2}\right)\right)}\right]\right)}{C(\upsilon)},
$$

for $\upsilon > 0$ and baseline parameter vector $\underline{\kappa}$,

$$
F(z;\underline{\kappa}) = 1-\left[\frac{\exp\left(-\left(\frac{G(z;\underline{\kappa})}{1-G(z;\underline{\kappa})}\right)^{2}\right)}{1+\left(1-\exp\left(-\left(\frac{G(z;\underline{\kappa})}{1-G(z;\underline{\kappa})}\right)^{2}\right)\right)}\right],
$$

for baseline parameter vector $\underline{\kappa}$, and

$$
F(z;\beta,\underline{\kappa}) = 1-\left[\frac{1-\mathrm{H}(z;\beta,\underline{\kappa})}{1+\mathrm{H}(z;\beta,\underline{\kappa})}\right],
$$

for $\beta > 0$ and $\underline{\kappa}$ being the baseline parameter vector, respectively.

2.2. Some statistical properties

Here we examine different mathematical characteristics of the TII-EHL-OBX-GPS CoD.

2.2.1. The Hazard rate function

Analyzing survival data relies significantly on the hrf, which provides essential information about the rate of failure over time. The hrf of TII-EHL-OBX-GPS CoD can be expressed as

$$\begin{aligned} h_{TII-EHL-OBX-G}(z;\beta,\upsilon,q,\underline{\kappa}) &= 4\beta\upsilon q\left(1-\mathrm{H}(z;\beta,\underline{\kappa})\right)^{q-1}\left(1+\mathrm{H}(z;\beta,\underline{\kappa})\right)^{-(q+1)} \\ &\times\left(1-\exp\left(-\left(\frac{G(z;\underline{\kappa})}{1-G(z;\underline{\kappa})}\right)^{2}\right)\right)^{\beta-1} \\ &\times\exp\left(-\left(\frac{G(z;\underline{\kappa})}{1-G(z;\underline{\kappa})}\right)^{2}\right)\left(1-G(z;\underline{\kappa})\right)^{-3}G(z;\underline{\kappa})g(z;\underline{\kappa}) \\ &\times\frac{C'\left(\upsilon\left[\frac{1-\mathrm{H}(z;\beta,\underline{\kappa})}{1+\mathrm{H}(z;\beta,\underline{\kappa})}\right]^{q}\right)}{C\left(\upsilon\left[\frac{1-\mathrm{H}(z;\beta,\underline{\kappa})}{1+\mathrm{H}(z;\beta,\underline{\kappa})}\right]^{q}\right)}, \end{aligned}$$

for $q,\beta,\upsilon>0$, $z>0$, and $\underline{\kappa}$ being the baseline parameter vector.

2.2.2. The quantile function (qf)

The qf for TII-EHL-OBX-GPS CoD can be derived by reversing the cdf of TII-EHL-OBX-GPS CoD, as indicated in the cdf referenced (2). Consequently, the qf for TII-EHL-OBX-GPS CoD is defined by

$$Q_G(u;q,\beta,\upsilon,\underline{\kappa}) = G^{-1}\left[\left(\left[-\log\left(1-\left(\frac{1-\left[\frac{C^{-1}(C(\upsilon)(1-u))}{\upsilon}\right]^{\frac{1}{q}}}{1+\left[\frac{C^{-1}(C(\upsilon)(1-u))}{\upsilon}\right]^{\frac{1}{q}}}\right)^{\frac{1}{\beta}}\right)\right]^{\frac{-1}{2}}+1\right)^{-1}\right], \tag{4}$$

for $0\le u\le 1$. As result, equation (4) can be used for simulations and to generate random numbers for the TII-EHL-OBX-GPS CoD, for any defined parent cdf $G(z;\underline{\kappa})$ and function $C(\upsilon)$.

2.2.3. Series representation of density function

In Sub-subsection 2.2.3, we introduce a series expansion for pdf of the TII-EHL-OBX-GPS CoD. Equation (3) can be expressed as an infinite linear combination of exponentiated-G (Exp-G) distributions, that is,

$$f_{TII-EHL-OBX-GPS}(z)=\sum_{h=0}^{\infty}C_{h+1}\,g_{h+1}(z;\underline{\kappa}),$$

where $g_{h+1}(z;\underline{\kappa})=(h+1)[G(z;\underline{\kappa})]^{h}g(z;\underline{\kappa})$ is an Exp-G distribution with parameter $(h+1)$ and parent parameter vector $\underline{\kappa}$, and

$$\begin{aligned} C_{h+1} &= \sum_{n=1}^{\infty}\sum_{k,i,w,l,u=0}^{\infty}(-1)^{k+i+w+u}\frac{na_n\upsilon^{n}}{C(\upsilon)l!}\binom{qn-1}{k}\binom{qn+i}{i}\binom{\beta(k+i+1)-1}{w} \\ &\times\binom{2l+1}{u}\binom{3+2l-u}{h}(-(w+1))^{l}\left(\frac{4q\beta\upsilon}{h+1}\right). \end{aligned} \tag{5}$$

Hence, the statistical and mathematical characteristics of the new distribution can be derived from those of the Exp-G distribution. Note that appendix section gives information on how the series representation of the pdf is derived.

2.2.4. The raw moments and Moment Generating Function (MGF)

The raw moments and MGF of TII-EHL-OBX-GPS CoD are presented in Sub-subsection 2.2.4, which characterize a probability distribution. Let $f_{TII-EHL-OBX-GPS}(z)$ be denoted by $f(z)$ and if $X_{h+1}\sim Exp-G(h+1,\underline{\kappa})$, the b^{th} raw moment is defined by

$$E(Z^{b})=\int_{-\infty}^{\infty}z^{b}f(z)dz=\sum_{h=0}^{\infty}C_{h+1}\,E(X_{h+1}^{b}),$$

where $E(X_{h+1}^{b})$ represent the b^{th} moment of X_{h+1} and C_{h+1} is defined in equation (5) When $|t|<1$, then the MGF, is given by:

$$M_Z(t) = \sum_{u=0}^{\infty} C_{h+1} M_{h+1}(t),$$

where $M_{h+1}(t)$ is the MGF of X_{h+1} and equation (5) define C_{h+1}.

2.2.5. The s^{th} order statistics

Order statistics are particularly valuable in estimating parameters and determining key measures like the median. For any given random sample $Z_1, Z_2, ..., Z_n$ from TII-EHL-OBX-GPS CoD and associated order statistics is $Z_{1:n} < Z_{2:n} \cdots < Z_{n:n}$, the s^{th} order statistic have pdf given as

$$f_{s:n}(z) = \frac{n!}{(s-1)!(n-s)!} \sum_{c=0}^{n-s} \sum_{h=0}^{\infty} \binom{n-s}{c} (-1)^c a_{h+1} g_{h+1}(z; \underline{\boldsymbol{\kappa}}),$$

where $g_{h+1}(z; \underline{\boldsymbol{\kappa}}) = (h+1)[G(z; \underline{\boldsymbol{\kappa}})]^h g(z; \underline{\boldsymbol{\kappa}})$ is the Exp-G distribution with the parameter $(h+1)$, and parameter vector $\underline{\boldsymbol{\kappa}}$, where

$$\begin{aligned} a_{h+1} = & \sum_{n,t=1}^{\infty} \sum_{p,k,i,w,l,u=0}^{\infty} \frac{d_{p,t} n a_n v^{n+t}}{(C(v))^{p+1} l!} \binom{s+c-1}{p} \binom{q(n+t)-1}{k} \\ & \times \binom{q(n+t)+i}{i} \binom{\beta(k+i)-1}{w} \binom{2l+1}{u} \\ & \times \binom{3+2l-u}{h} (-1)^{p+k+i+w+u} (-(w+1))^l \left(\frac{4q\beta v}{h+1}\right). \end{aligned}$$

2.2.6. Rényi entropy

Entropy quantifies degree of variability associated with a random variable. Rényi entropy [34], broadens the scope of Shannon entropy and it can be defined as

$$I_R(\rho) = \frac{1}{1-\rho} \log \left(\int_0^{\infty} [f(z)]^{\rho} dz \right), \rho \neq 1, \rho > 0.$$

The Rényi entropy for the TII-EHL-OBX-GPS CoD is

$$I_R(\rho) = \frac{1}{1-\rho} \log \left[\sum_{h=0}^{\infty} \tau_h \exp\left((1-\rho) I_{REG} \right) \right], \rho \neq 1, \rho > 0,$$

where $I_{REG} = \frac{1}{1-\rho} \log \left[\int_0^{\infty} \left(\left[1 + \frac{h}{\rho}\right] \left(G(z; \underline{\boldsymbol{\kappa}})\right)^{\frac{h}{\rho}} \left(g(z; \underline{\boldsymbol{\kappa}})\right) \right)^{\rho} dy \right]$ is the Rényi entropy of an Exp-G distribution with parameter $(1 + \frac{h}{\rho})$ and

$$\begin{aligned} \tau_h = & \sum_{n=1}^{\infty} \sum_{k,i,w,l,u=0}^{\infty} \frac{n d_{\rho,n} v^{\rho+n-1}}{(C(v))^{\rho} l!} \binom{q(n+\rho-1)-\rho}{k} \binom{(q(\rho+n-1)+\rho)+i-1}{i} \\ & \times \binom{\beta(\rho+k+i)-\rho}{w} \binom{2l+\rho}{u} \binom{3\rho+2l-u}{h} (-1)^{k+i+w+u} (-(\rho+w))^l \frac{(4q\beta)^{\rho}}{\left[1+\frac{h}{\rho}\right]^{\rho}}. \end{aligned}$$

Hence, Rényi entropy of the TII-EHL-OBX-GPS CoD is derived based on the Rényi entropy of the Exp-G distribution. Details on the derivations is given in the Appendix.

3. Some cases

The special classes of the TII-EHL-OBX-GPS CoD are presented in Section 3. We take into account two PS distributions, the Poisson distribution and logarithmic distribution, and take Weibull and log-logistic distributions as parent distributions. The log-logistic distribution have cdf and pdf defined by $G(z; c) = 1 - (1 + z^c)^{-1}$ and $g(z; c) = c z^{c-1}(1 + z^c)^{-2}$, for $c > 0$ and $z > 0$. The Weibull distribution have cdf and pdf defined by $G(z; \lambda) = 1 - e^{-z^{\lambda}}$ and $g(z; \lambda) = \lambda z^{\lambda-1} e^{-z^{\lambda}}$, for $\lambda > 0$ and $z > 0$.

3.1. Type II exponentiated half logistic-odd Burr X-Weibull Logarithmic (TII-EHL-OBX-WL) distribution

In subsection 3.1, we introduce the TII-EHL-OBX-WL distribution and present the pdf and hrf plots. Additionally, we include the 3D plots of SK and KS. The cdf of TII-EHL-OBX-WL distribution can be written as

$$F_{TII-EHL-OBX-WL}(z) = 1 - \frac{-\log\left(1 - v\left[\frac{1-\mathrm{H}(z;\beta,\lambda)}{1+\mathrm{H}(z;\beta,\lambda)}\right]^q\right)}{-\log(1-v)}.$$

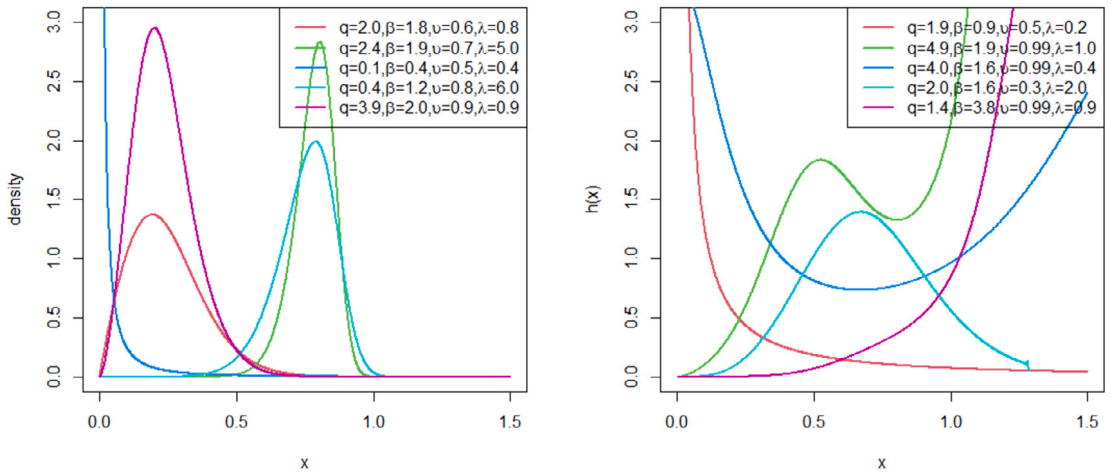

Fig. 1. Illustrations of the (a) Pdf and (b) Hrf Plots for TII-EHL-OBX-WL Distribution.

The pdf and hrf are

$$f_{TII-EHL-OBX-WL}(z) = 4q\beta\upsilon\left(\mathrm{H}(z;\beta,\lambda)\right)^{q-1}\left(1+\mathrm{H}(z;\beta,\lambda)\right)^{-(q+1)} \times\left(1-\exp\left(-\left(\frac{G(z;\lambda)}{1-G(z;\lambda)}\right)^{2}\right)\right)^{\beta-1}\exp\left(-\left(\frac{G(z;\lambda)}{1-G(z;\lambda)}\right)^{2}\right) \times\left(1-G(z;\lambda)\right)^{-3}\left(G(z;\lambda)\right)g(z;\lambda)\frac{\left(1-\upsilon\left[\frac{1-\mathrm{H}(z;\beta,\lambda)}{1+\mathrm{H}(z;\beta,\lambda)}\right]^{q}\right)^{-1}}{-\log(1-\upsilon)},$$

and

$$h_{TII-EHL-OBX-WL}(z) = 4q\beta\upsilon\left(1-\mathrm{H}(z;\beta,\lambda)\right)^{q-1}\left(1+\mathrm{H}(z;\beta,\lambda)\right)^{-(q+1)} \times\left(1-\exp\left(-\left(\frac{G(z;\lambda)}{1-G(z;\lambda)}\right)^{2}\right)\right)^{\beta-1}\exp\left(-\left(\frac{G(z;\lambda)}{1-G(z;\lambda)}\right)^{2}\right) \times\left(1-G(z;\lambda)\right)^{-3}\left(G(z;\lambda)\right)g(z;\lambda)\frac{\left(1-\upsilon\left[\frac{1-\mathrm{H}(z;\beta,\lambda)}{1+\mathrm{H}(z;\beta,\lambda)}\right]^{q}\right)^{-1}}{-\log\left(1-\upsilon\left[\frac{1-\mathrm{H}(z;\beta,\lambda)}{1+\mathrm{H}(z;\beta,\lambda)}\right]^{q}\right)},$$

respectively, where $\mathrm{H}(z;\beta,\lambda)=\left(1-\exp\left(-\left(\frac{G(z;\lambda)}{1-G(z;\lambda)}\right)^{2}\right)\right)^{\beta}$, for $0<\upsilon<1$ and $z,q,\lambda,\beta>0$. In reference to the TII-EHL-OBX-WL distribution, Fig. 1 provides visual representations of both the pdf and hrf. This density function can accommodate uni-modal, negative-skewed or positive-skewed, and reverse-J shapes, whereas hrf plots can accommodate different shapes including monotonic and non-monotonic. Figs. 2 and 3 depicts the SK and KS plots for the TII-EHL-OBX-WL distribution.

- If we hold λ and υ constant while increasing β and q, we get a highly skewed and platykurtic KS.
- If υ and β are fixed, increasing q and λ results in an increase in SK and KS.

3.2. Type II exponentiated half logistic-odd Burr X-Weibull Poisson (TII-EHL-OBX-WP) distribution

In subsection 3.2, we present the pdf and hrf plots, as well as three dimensional plots of SK and KS. The cdf is

$$F_{TII-EHL-OBX-WP}(z) = 1-\frac{\exp\left(\upsilon\left[\frac{1-\mathrm{H}(z;\beta,\lambda)}{1+\mathrm{H}(z;\beta,\lambda)}\right]^{q}\right)-1}{\exp(\upsilon)-1}.$$

The pdf is

$$f_{TII-EHL-OBX-WP}(z) = 4q\beta\upsilon\left(1-\mathrm{H}(z;\beta,\lambda)\right)^{q-1}\left(1+\mathrm{H}(z;\beta,\lambda)\right)^{-(q+1)}$$

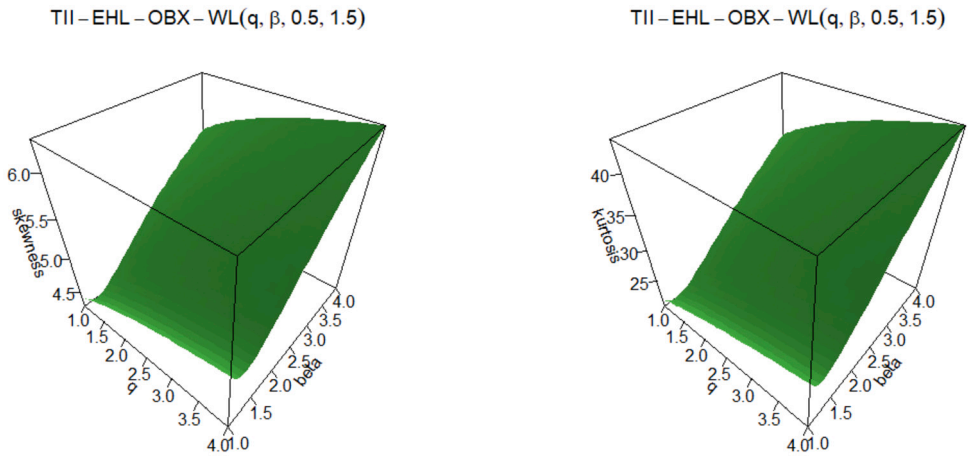

Fig. 2. SK and KS Plots of TII-EHL-OBX-WL Distribution.

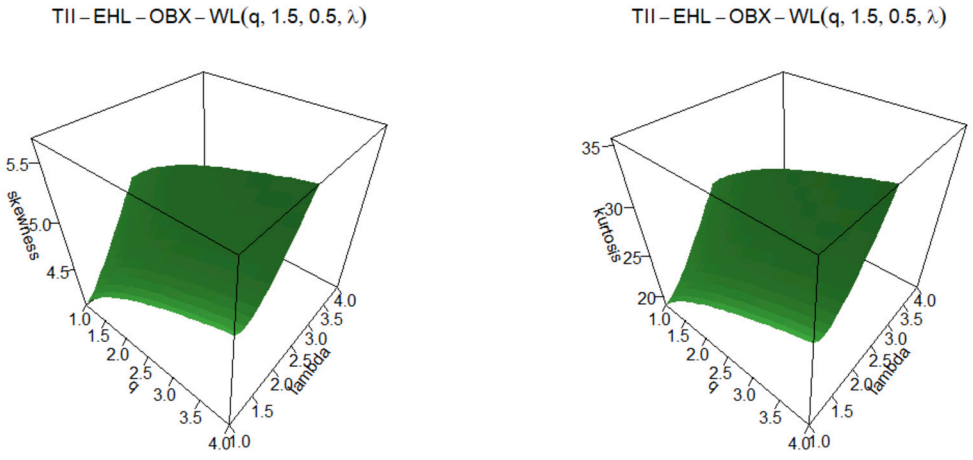

Fig. 3. SK and KS Plots of TII-EHL-OBX-WL Distribution.

$$\times\left(1-\exp\left(-\left(\frac{G(z;\lambda)}{1-G(z;\lambda)}\right)^2\right)\right)^{\beta-1}\exp\left(-\left(\frac{G(z;\lambda)}{1-G(z;\lambda)}\right)^2\right)$$
$$\times\left(1-G(z;\lambda)\right)^{-3}\left(G(z;\lambda)\right)g(z;\lambda)\frac{\exp\left(\upsilon\left[\frac{1-\mathrm{H}(z;\beta,\lambda)}{1+\mathrm{H}(z;\beta,\lambda)}\right]^q\right)}{\exp(\upsilon)-1},$$

where $\mathrm{H}(z;\beta,\lambda)=\left(1-\exp\left(-\left(\frac{G(z;\lambda)}{1-G(z;\lambda)}\right)^2\right)\right)^{\beta}$ for $z,q,\beta,\lambda,\upsilon>0$. The hrf is

$$h_{TII-EHL-OBX-WP}(z)=4q\beta\upsilon\left(1-\mathrm{H}(z;\beta,\lambda)\right)^{q-1}\left(1+\mathrm{H}(z;\beta,\lambda)\right)^{-(q+1)}$$
$$\times\left(1-\exp\left(-\left(\frac{G(z;\lambda)}{1-G(z;\lambda)}\right)^2\right)\right)^{\beta-1}\exp\left(-\left(\frac{G(z;\lambda)}{1-G(z;\lambda)}\right)^2\right)$$
$$\times\left(1-G(z;\lambda)\right)^{-3}\left(G(z;\lambda)\right)g(z;\lambda)\frac{\exp\left(\upsilon\left[\frac{1-\mathrm{H}(z;\beta,\lambda)}{1+\mathrm{H}(z;\beta,\lambda)}\right]^q\right)}{\exp\left(\upsilon\left[\frac{1-\mathrm{H}(z;\beta,\lambda)}{1+\mathrm{H}(z;\beta,\lambda)}\right]^q\right)-1}$$

for $z,q,\beta,\lambda,\upsilon>0$.

Fig. 4 provides graphical representations of both the density function and hrf for the TII-EHL-OBX-WP distribution. The density function can accommodate different shapes such as symmetric, reverse-J, positive-skewed or negative-skewed. Moreover, the hrf can accommodate different form including monotonic and non monotonic. The SK and KS plots for the TII-EHL-OBX-WP distribution are depicted in Figs. 5 and 6.

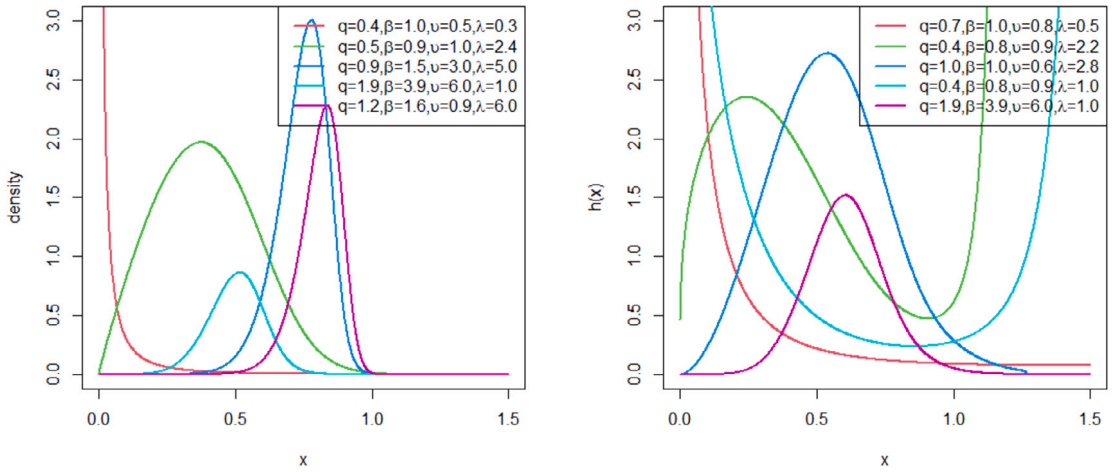

(a) (b)

Fig. 4. Illustrations of the (a) Pdf and (b) Hrf Plots of TII-EHL-OBX-WP Distribution.

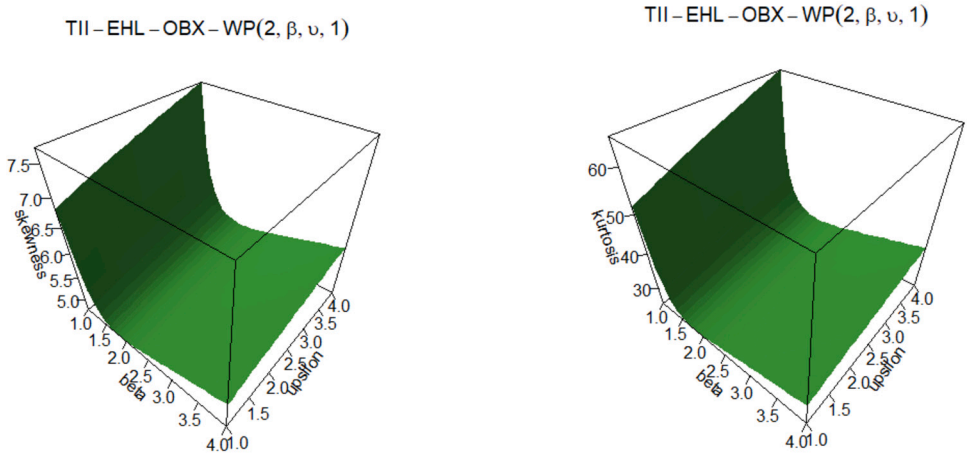

Fig. 5. SK and KS Plots of TII-EHL-OBX-WP Distribution.

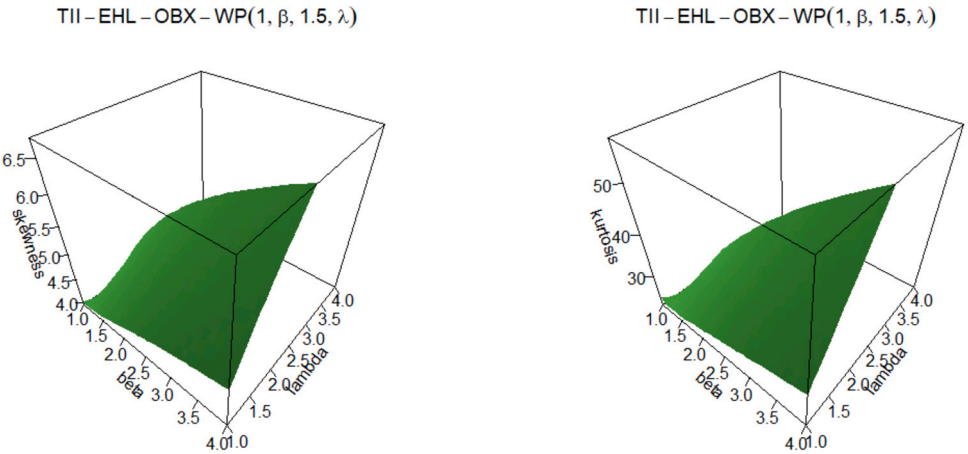

Fig. 6. SK and KS Plots of TII-EHL-OBX-WP Distribution.

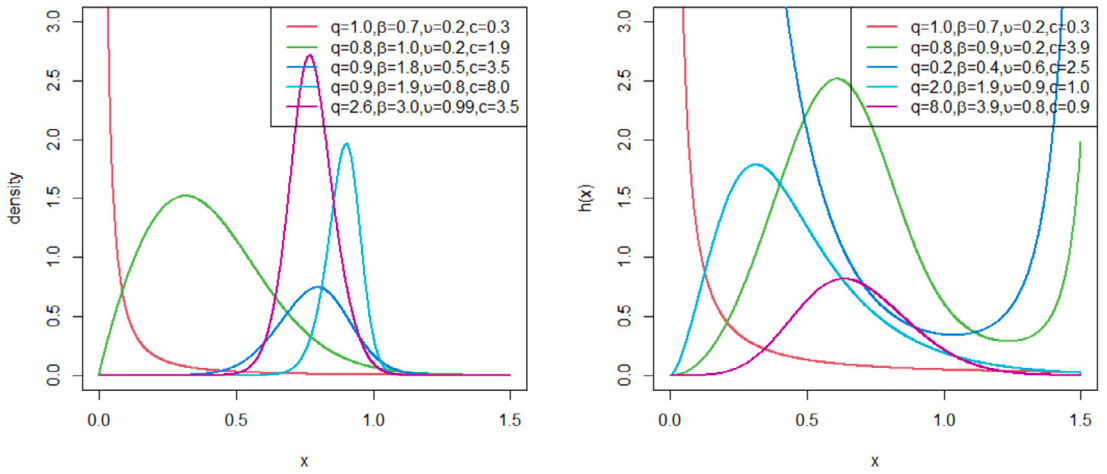

(a) (b)

Fig. 7. Illustrations of the (a) Pdf and (b) Hrf Plots of TII-EHL-OBX-LLoGL Distribution.

- When the model parameters λ and q are held fixed, the decrease of SK and KS coincides with increase in β and υ.
- When the model parameters q and υ are fixed, the SK and KS increase then decrease while β and λ increase.

3.3. Type II exponentiated half logistic-odd Burr X-Log-Logistic Logarithmic (TII-EHL-OBX-LLoGL) distribution

Subsection 3.3, presents the cdf, pdf, hrf of TII-EHL-OBX-LLoGL distribution. The pdf and hrf plots, as well as the 3D plots of SK and KS, are presented. The cdf of the TII-EHL-OBX-LLoGL distribution is given by

$$F_{TII-EHL-OBX-LLoGL}(z) = 1 - \frac{-\log\left(1-\upsilon\left[\frac{1-\mathrm{H}(z;\beta,c)}{1+\mathrm{H}(z;\beta,c)}\right]^{q}\right)}{-\log(1-\upsilon)},$$

the pdf is

$$\begin{aligned} f_{TII-EHL-OBX-LLoGL}(z) &= 4q\beta\upsilon(1-\mathrm{H}(z;\beta,c))^{q-1}(1+\mathrm{H}(z;\beta,c))^{-(q+1)} \\ &\times\left(1-\exp\left(-\left(\frac{G(z;c)}{1-G(z;c)}\right)^{2}\right)\right)^{\beta-1} \\ &\times\exp\left(-\left(\frac{G(z;c}{1-G(z;c)}\right)^{2}\right)(1-G(z;c))^{-3}(G(z;c)) \\ &\times g(z;c)\frac{\left(1-\upsilon\left[\frac{1-\mathrm{H}(z;\beta,c)}{1+\mathrm{H}(z;\beta,c)}\right]^{q}\right)^{-1}}{-\log(1-\upsilon)}, \end{aligned}$$

and the hrf is

$$\begin{aligned} h_{TII-EHL-OBX-LLoGL}(z) &= 4q\beta\upsilon(1-\mathrm{H}(z;\beta,c))^{q-1}(1+\mathrm{H}(z;\beta,c))^{-(q+1)} \\ &\times\left(1-\exp\left(-\left(\frac{G(z;c)}{1-G(z;c)}\right)^{2}\right)\right)^{\beta-1} \\ &\times\exp\left(-\left(\frac{G(z;c)}{1-G(z;c)}\right)^{2}\right)(1-G(z;c))^{-3}(G(z;c)) \\ &\times g(z;c)\frac{\left(1-\upsilon\left[\frac{1-\mathrm{H}(z;\beta,c)}{1+\mathrm{H}(z;\beta,c)}\right]^{q}\right)^{-1}}{-\log\left(1-\upsilon\left[\frac{1-\mathrm{H}(z;\beta,c)}{1+\mathrm{H}(z;\beta,c)}\right]^{q}\right)}, \end{aligned}$$

respectively, where $\mathrm{H}(z;\beta,c) = \left(1-\exp\left(-\left(\frac{G(z;c)}{1-G(z;c)}\right)^{2}\right)\right)^{\beta}$, for $0<\upsilon<1$ and $z,q,\beta,c>0$.

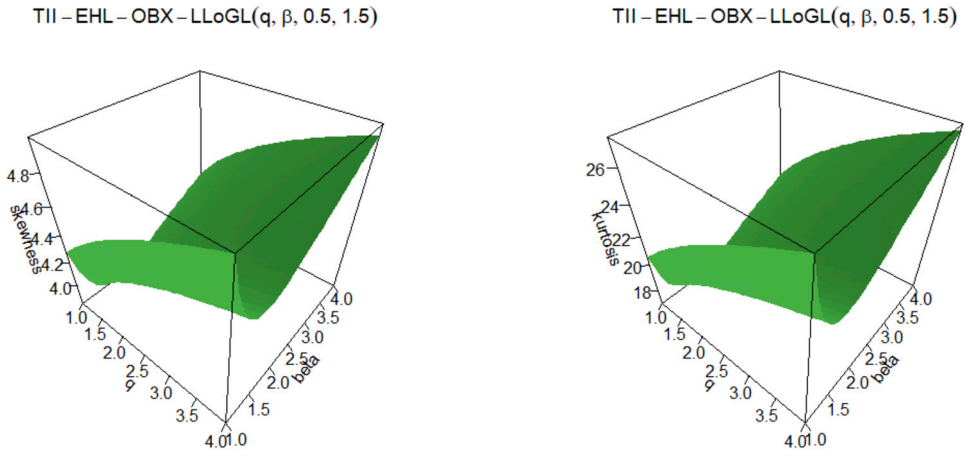

Fig. 8. SK and KS Plots of TII-EHL-OBX-LLoGL Distribution.

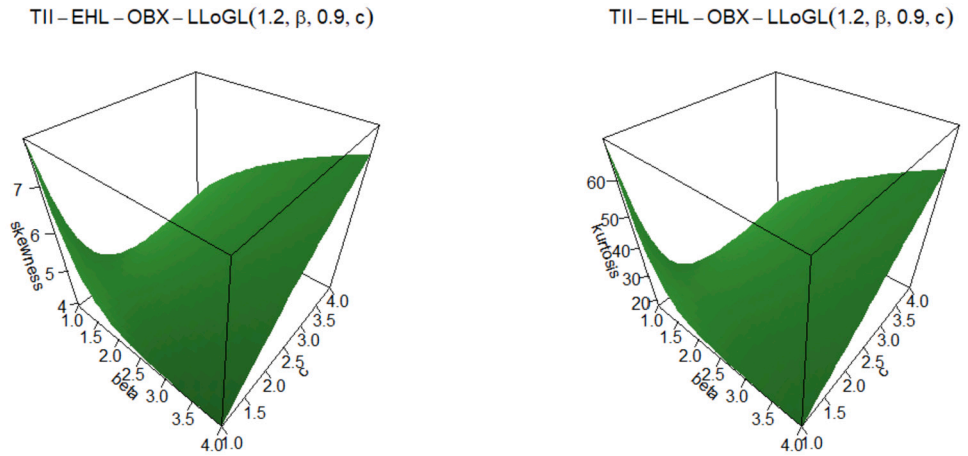

Fig. 9. SK and KS Plots of TII-EHL-OBX-LLoGL Distribution.

The graphical representation illustrating the pdf and hrf of TII-EHL-OBX-LLoGL distribution are showcased in Fig. 7. The density function accommodate different forms such as uni-modal, negatively or positively skewed, and reverse-J. The hrf can be monotonic or non-monotonic in shape. The SK and KS plots for TII-EHL-OBX-LLoGL distribution are shown in Figs. 8 and 9, respectively.

- When the parameters υ and c are fixed, the SK and KS decrease and then increase, while q and β increase,
- When q and υ are fixed, the SK and KS increase as β and c increase.

3.4. Type II exponentiated half logistic-odd Burr X-Log-Logistic Poisson (TII-EHL-OBX-LLoGP) distribution

In subsection 3.4, we present the pdf and hrf plots, as well as 3D plots of SK and KS. The cdf and pdf are

$$F_{TII-EHL-OBX-LLoGP}(z) = 1 - \frac{\exp\left(\upsilon\left[\frac{1-\mathrm{H}(z;\beta,c)}{1+\mathrm{H}(z;\beta,c)}\right]^{q}\right) - 1}{\exp(\upsilon - 1)}$$

and

$$f_{TII-EHL-OBX-LLoGP}(z) = 4q\beta\upsilon(1-\mathrm{H}(z;\beta,c))^{q-1}(1+\mathrm{H}(z;\beta,c))^{-(q+1)} \times \left(1-\exp\left(-\left(\frac{G(z;c)}{(1-G(z;c)}\right)^{2}\right)\right)^{\beta-1} \times \exp\left(-\left(\frac{G(z;c)}{1-G(z;c)}\right)^{2}\right)(1-G(z;c))^{-3}$$

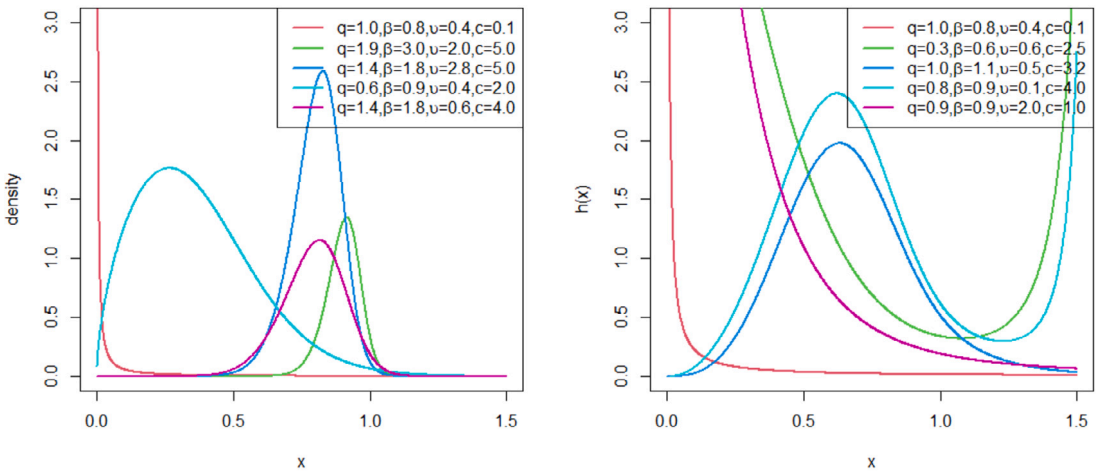

(a) (b)

Fig. 10. Illustrations of the (a) Pdf and (b) Hrf Plots of TII-EHL-OBX-LLoGP Distribution.

$$\times (G(z;c))\, g(z;c) \frac{\exp\left(\upsilon\left[\frac{1-\mathrm{H}(z;\beta,c)}{1+\mathrm{H}(z;\beta,c)}\right]^q\right)}{\exp(\upsilon)-1},$$

and the hrf is

$$\begin{aligned} h_{TII-EHL-OBX-LLoGP}(z) &= 4q\beta\upsilon\,(1-\mathrm{H}(z;\beta,c))^{q-1}\,(1+\mathrm{H}(z;\beta,c))^{-(q+1)} \\ &\times \left(1-\exp\left(-\left(\frac{G(z;c)}{1-G(z;c)}\right)^2\right)\right)^{\beta-1} \\ &\times \exp\left(-\left(\frac{G(z;c)}{1-G(z;c)}\right)^2\right)(1-G(z;c))^{-3} \\ &\times (G(z;c))\, g(z;c) \frac{\exp\left(\upsilon\left[\frac{1-\mathrm{H}(z;\beta,c)}{1+\mathrm{H}(z;\beta,c)}\right]^q\right)}{\exp\left(\upsilon\left[\frac{1-\mathrm{H}(z;\beta,c)}{1+\mathrm{H}(z;\beta,c)}\right]^q\right)-1}, \end{aligned}$$

where $\mathrm{H}(z;\beta,c) = \left(1-\exp\left(-\left(\frac{G(z;c)}{1-G(z;c)}\right)^2\right)\right)^{\beta}$ for $z,q,\upsilon,\beta,c>0$. The plots of the pdf in Fig. 10 show positively or negatively skewed, reverse-J and uni-modal shapes. Moreover, the hrf shown in Fig. 10 accommodate different shapes, including monotonic and non-monotonic. The SK and KS plots for the TII-EHL-OBX-LLoGP distribution are shown in Figs. 11 and 12.

- If we fix β and υ, parameter q and c increase as SK decrease and KS increase, and
- If we fix q and c, parameter β and υ increase as SK and KS increase.

4. Maximum likelihood estimation

Let $Z \sim$ TII-EHL-OBX-GPS $(q,\upsilon,\beta,\underline{\boldsymbol{\kappa}})$ and the vector of parameters represented by $\boldsymbol{\Omega} = (q,\upsilon,\beta,\underline{\boldsymbol{\kappa}})^T$. For any given random sample of size n from the TII-EHL-OBX-GPS CoD, the log-likelihood function is given by

$$\begin{aligned} \ell_n(\boldsymbol{\Omega}) &= n\ln(4q\beta\upsilon) + (q-1)\sum_{i=1}^{n}\ln\left(1-\mathrm{H}(z;\beta,\underline{\boldsymbol{\kappa}})\right) - (q+1)\sum_{i=1}^{n}\ln\left(1+\mathrm{H}(z;\beta,\underline{\boldsymbol{\kappa}})\right) \\ &+ (\beta-1)\sum_{i=1}^{n}\ln\left(1-\exp\left(-\left(\frac{G(z;\underline{\boldsymbol{\kappa}})}{1-G(z;\underline{\boldsymbol{\kappa}})}\right)^2\right)\right) \\ &+ \sum_{i=1}^{n}\left(-\left(\frac{G(z;\underline{\boldsymbol{\kappa}})}{1-G(z;\underline{\boldsymbol{\kappa}})}\right)^2\right) - 3\sum_{i=1}^{n}\ln\left(1-G(z_i;\underline{\boldsymbol{\kappa}})\right) \end{aligned}$$

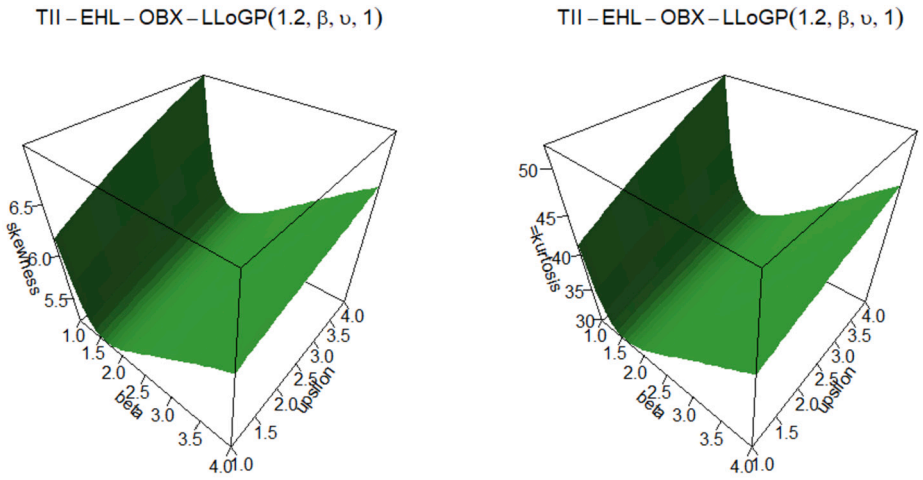

Fig. 11. SK and KS Plots of TII-EHL-OBX-LLoGP Distribution.

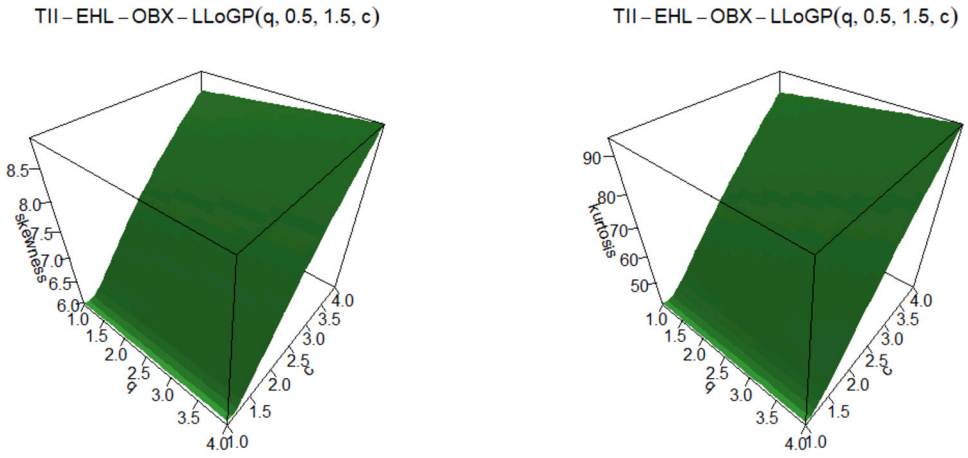

Fig. 12. SK and KS Plots of TII-EHL-OBX-LLoGP Distribution.

$$+\sum_{i=1}^{n}\ln\left(g(z_i;\underline{\kappa})\right)+\sum_{i=1}^{n}\ln\left[\frac{C'\left(\upsilon\left[\frac{1-\mathrm{H}(z;\beta,\underline{\kappa})}{1+\mathrm{H}(z;\beta,\underline{\kappa})}\right]^{q}\right)}{C(\upsilon)}\right]+\sum_{i=1}^{n}\ln\left(G(z_i;\underline{\kappa})\right),$$

when $\mathrm{H}(z;\beta,\underline{\kappa})=\left(1-exp\left(-\left(\frac{G(z;\underline{\kappa})}{1-G(z;\underline{\kappa})}\right)^{2}\right)\right)^{\beta}$ The elements of the score vector $U=\left(\frac{\partial\ell}{\partial q},\frac{\partial\ell}{\partial\beta},\frac{\partial\ell}{\partial\upsilon},\frac{\partial\ell}{\partial\underline{\kappa}_k}\right)$ are given in the Appendix.

5. Monte Carlo simulation study

The consistency of the TII-EHL-OBX-LLoGP distribution is investigated in this section by running several simulations for various sample sizes (n) including 25, 50, 100, 200, 400, 800 and 1600. We performed simulations for a total of 1000 samples. Tables 2 and 3 presents the simulation results for selected sets of parameter values. Evaluating the precision of MLEs involves using metrics like mean of MLEs, average bias (ABias), and root mean square error (RMSE).

According to the results obtained from the simulation experiments, as the n increases, the mean parameter estimates converge towards the actual parameter values. In addition, as the n increases, the ABias and RMSE decrease. Therefore, the estimates of the TII-EHL-OBX-LLoGP distribution are consistent.

6. Data analysis

The applicability and suitability of the TII-EHL-OBX-LLoGP distribution are demonstrated by fitting the model to agriculture data, survival years data and carbon fibres data.

Table 2
MCS Results for TII-EHL-OBX-LLoGP Distribution.

parameter	n	Mean	(0.5,2.8,0.5,1.0) RMSE	ABias	Mean	(0.5,0.9,0.5,1.0) RMSE	ABias
q	25	1.3605	5.0589	0.8605	2.0199	8.5869	1.5199
	50	1.2565	3.2502	0.7565	1.4087	4.0829	0.9087
	100	1.1125	2.5127	0.6125	1.1045	2.1146	0.6045
	200	0.8615	1.3155	0.3615	0.8660	1.2878	0.3660
	400	0.7363	1.0408	0.2363	0.7621	1.0430	0.2621
	800	0.6895	0.7804	0.1895	0.6489	0.7208	0.1489
	1600	0.5691	0.4983	0.0691	0.5831	0.5454	0.0831
β	25	2.7703	0.5943	-0.0296	0.8904	0.2074	-0.0095
	50	2.7903	0.4841	-0.0096	0.8842	0.1577	-0.0157
	100	2.8009	0.3866	0.0009	0.8764	0.1213	-0.0235
	200	2.8100	0.3046	0.0100	0.8791	0.0884	-0.0208
	400	2.8267	0.2438	0.0267	0.8919	0.0729	-0.0080
	800	2.8237	0.1943	0.0237	0.8948	0.0599	-0.0051
	1600	2.8055	0.1601	0.0055	0.8986	0.0463	-0.0013
υ	25	1.2611	1.3803	0.7611	1.2405	1.3557	0.7405
	50	0.9634	1.0678	0.4634	1.0281	1.1216	0.5281
	100	0.8848	0.9724	0.3849	0.8877	0.9992	0.3877
	200	0.8369	0.8309	0.3369	0.8639	0.8744	0.3639
	400	0.7992	0.7305	0.2992	0.8098	0.7751	0.3098
	800	0.7056	0.6192	0.2056	0.6829	0.5629	0.1829
	1600	0.5735	0.5316	0.0735	0.5333	0.4224	0.0333
c	25	2.2890	2.6525	1.2890	0.9472	1.5640	-0.0527
	50	1.8637	2.0721	0.8637	1.2196	1.6489	0.2196
	100	1.5366	1.5752	0.5366	1.3502	1.6212	0.3502
	200	1.4080	1.2624	0.4080	1.4031	1.6911	0.4031
	400	1.3146	0.9489	0.3146	1.3116	1.3843	0.3116
	800	1.3014	0.7900	0.3014	1.1574	0.9204	0.1574
	1600	1.2761	0.6236	0.2761	1.0270	0.7478	0.0270

Table 3
MCS Results for TII-EHL-OBX-LLoGP Distribution.

parameter	n	Mean	(2.0, 0.2, 0.2, 1.5) RMSE	ABias	Mean	(1.5, 2.0, 0.5, 0.2) RMSE	ABias
q	25	2.3242	1.5995	0.3242	1.7769	2.0527	0.2769
	50	2.2891	0.7258	0.2891	1.6470	0.7493	0.1470
	100	2.1802	0.5130	0.1802	1.6279	0.5448	0.1279
	200	2.1297	0.3761	0.1297	1.5950	0.3804	0.0950
	400	2.0810	0.2470	0.0810	1.5760	0.2833	0.0760
	800	2.0302	0.1698	0.0302	1.5407	0.1867	0.0407
	1600	2.0203	0.1185	0.0203	1.5255	0.1297	0.0255
β	25	0.2946	0.2456	0.0946	2.9536	9.0485	0.9536
	50	0.2344	0.1002	0.0344	2.0187	1.1005	0.0187
	100	0.2152	0.0612	0.0152	2.0173	0.4307	0.0173
	200	0.2106	0.0485	0.0106	2.0011	0.5098	0.0011
	400	0.2106	0.0485	0.0106	1.9759	0.2755	-0.0240
	800	0.2025	0.0246	0.0025	1.9728	0.7297	-0.0271
	1600	0.1998	0.0177	-0.0001	1.9966	0.1978	-0.0033
υ	25	1.3933	4.5958	1.1933	1.0524	1.3065	0.5524
	50	0.5417	3.8791	0.3417	1.0538	1.1937	0.5538
	100	0.2104	0.1985	0.0104	1.0086	1.2306	0.5086
	200	0.2032	0.0578	0.0030	0.8188	0.9553	0.3188
	400	0.2002	0.0384	0.0002	0.7280	0.8316	0.2280
	800	0.1998	0.1423	-0.0001	0.6212	0.5987	0.1212
	1600	0.1989	0.0282	-0.0010	0.5588	0.3911	0.0588
c	25	2.4801	1.9519	0.9801	0.3593	0.3993	0.1593
	50	2.4262	1.9441	0.9262	0.2700	0.2034	0.0700
	100	1.9922	1.2245	0.4922	0.2516	0.1366	0.0516
	200	1.8972	0.9860	0.3972	0.2408	0.1334	0.0408
	400	1.7305	0.6389	0.2305	0.2194	0.0681	0.0194
	800	1.5996	0.4048	0.0996	0.2047	0.0276	0.0047
	1600	1.5500	0.2771	0.0500	0.2011	0.0170	0.0011

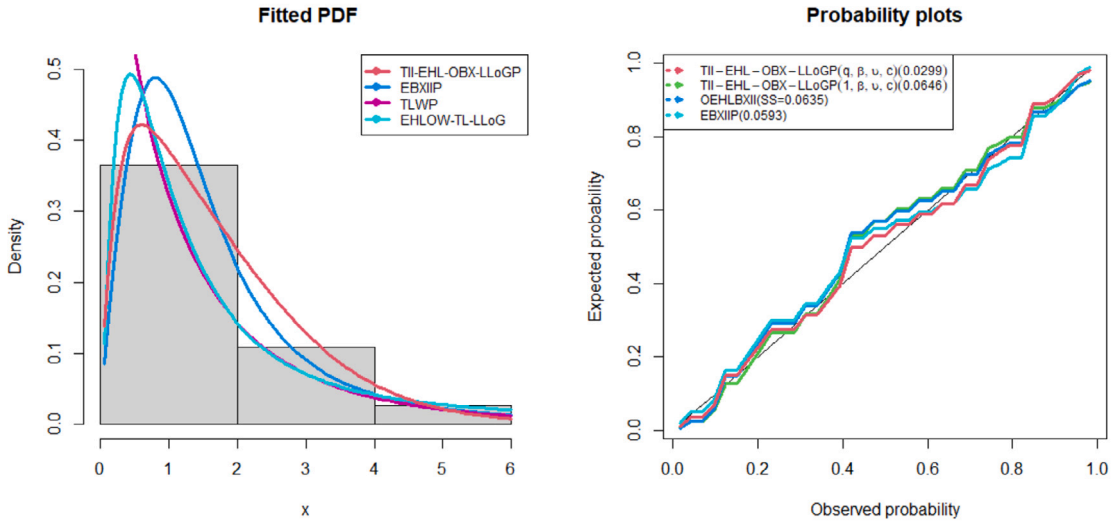

(a) (b)

Fig. 13. Fitted (a) Pdf and (b) PP Plots for Agriculture Data.

To determine the suitability of the model, we employed the AdequacyModel package. The function for **goodness.fit**() includes important statistics for assessing the suitability of lifetime probability models, including the -2loglikelihood ($-2\ell_n$), Anderson-Darling (AD), Cramér-von Mises (CVM), bayesian information criterion (BIC), consistent akaike information criterion (CAIC) and akaike information criterion (AIC) statistics. The sum of squares (SS) from probability plots (PP) and the Kolmogorov-Smirnov (K-S) statistic, as well as its associated p-value have been employed to evaluate goodness-of-fit (GoF) statistics. The most suitable distribution is determined by the least values of GoF statistics and K-S statistic with the largest p-value.

The Total Time on Test (TTT) graph proposed by [1] represent the behavior of hrf over time. The hrf is constant when it is straight diagonal, decreasing when it is convex, and increasing when it is concave. If the hrf has a bathtub shape, then it is initially convex followed concave. If the hrf is an upside-down bathtub, it starts with a concave and transitions to a convex shape.

The TII-EHL-OBX-LLoGP distribution was set in contrast to both nested and several non-nested equi-parameter distributions. The non-nested equi-parameter distributions considered are the generalized Gompertz-Poisson (GGP) distribution [39], odd exponentiated half logistic Burr XII (OEHLBXII) distribution [2], Topp-Leone generated Weibull (TLWP) distribution [21], exponentiated Burr-XII Poisson (EBXIIP) distribution [12], exponentiated half logistic odd Weibull-Topp-Leone-log-logistic (EHLOW-TL-LLoG) distribution [9] and odd power generalised Weibull-Weibull Poisson (OPGW-WP) distribution Oluyede et al. [31].

6.1. Agriculture data

The first data set depicts total factor productivity growth in agricultural production from 2001 to 2010 for thirty-seven African countries. This data was obtained from https://dataverse.harvard.edu/dataset.xhtml?PersistentId=doi:10.7910/DVN/9IOAKR, accessed 30 June 2022 and data points are given in appendix.

The estimated variance-covariance (Var-Cov) is

$$\begin{pmatrix} 6.8114\times10^{-07} & 3.2909\times10^{-04} & -4.3638\times10^{-08} & 1.2861\times10^{-04} \\ 3.2909\times10^{-04} & 0.2241 & 2.8547\times10^{-05} & -0.0672 \\ -4.3638\times10^{-08} & 2.8547\times10^{-05} & 3.6670\times10^{-09} & 9.1064\times10^{-06} \\ 1.2861\times10^{-04} & -0.0672 & 9.1064\times10^{-06} & 0.0295 \end{pmatrix}$$

and the estimated 95% confidence interval (CI) for q, υ, β and c are respectively, given as 0.0019 ± 0.0061, 0.9883 ± 0.9279, 147.9200 ± 0.0001 and 0.8186 ± 0.3366. In contrast to the competing distributions presented in Table 4, the agriculture data fit very well with TII-EHL-OBX-LLoGP distribution as it has least GoF statistics values, and the highest p-value for the K-S statistic. Fig. 13 showcase that the fitted graphical representations clearly indicate that the TII-EHL-OBX-LLoGP distribution outperforms several equi-parameter models used for comparison in fitting the agriculture data. Fig. 14 depicts the TTT plot for agriculture data, indicating a decreasing hrf. The Kaplan-Meier (K-M) along with the empirical cumulative distribution function (ECDF) curves for agriculture data are depicted in Fig. 15. Based on the closeness of the observed and fitted lines in Fig. 15, we observe that TII-EHL-OBX-LLoGP fit the agriculture data well. We exhibit the log-likelihood profile plot of the MLEs of the TII-EHL-OBX-LLoGP parameters for agriculture data in Fig. 16. The MLEs for TIIEHL-OBX-LLoGP distribution from agriculture data exist and can be achieved uniquely as shown in Fig. 16.

Table 4
Parameter Estimates and GoF Statistics for Agriculture Data.

	Estimates				Statistics								
Model	q	β	υ	c	$-2\log\hat{}$	AIC	$AICC$	BIC	CVM	AD	$K-S$	$P-VALUE$	SS
$TII-EHL-OBX-LLoGP(q,\beta,\upsilon,c)$	0.0019 (0.0008)	0.9883 (0.4734)	147.9200 (6.0556×10^{-05})	0.8186 (0.1717)	107.3051	115.3051	116.3324	121.5261	0.0340	0.2067	0.0829	0.9611	0.0299
$TII-EHL-OBX-LLoGP(1,\beta,\upsilon,c)$	- -	3.1295 (0.4515)	5.6664×10^{-08} (0.0323)	0.3847 (0.0471)	116.2720	122.2720	122.9993	127.1047	0.0711	0.4437	0.1321	0.5387	0.0646
$TII-EHL-OBX-LLoGP(1,1,\upsilon,c)$	- -	- -	3.1280×10^{-08} (0.0222)	0.4579 (0.0504)	158.1039	162.1038	162.4596	165.3258	0.0405	0.2493	0.4996	1.9000×10^{-08}	3.8789
EBXIIP	c 2.2169 (1.1973)	s 1.4832 (1.0731)	α 0.8275 (0.8693)	λ 7.7387×10^{-09} (0.0153)	110.6733	118.6733	119.9233	125.1169	0.0675	0.4191	0.1281	0.5783	0.0593
GGP	θ 0.5761 (0.9416)	α 3.9170 (2.5161)	β 1.2041 (0.3968)	γ 8.6309×10^{-09} (0.1199)	122.0838	130.0831	131.3331	136.5268	0.0379	0.2362	0.1959	0.1166	0.3159
TLWP	α 0.5392 (0.1271)	β 0.7452 (0.1231)	λ 1.3930 (0.3237)	θ 1.0019×10^{-08} (0.0233)	120.1369	128.1372	129.3872	134.5808	0.0421	0.2605	0.2732	0.0079	2.6874
OEHLBXII	α 0.1563 (0.0654)	λ 0.0148 (0.0372)	a 8.2485 (3.6295)	b 0.4037 (0.1418)	112.5454	120.5454	121.7954	126.9891	0.0533	0.2972	0.1257	0.6023	0.0635
EHLOW-TL-LLoG	b 56.7327 (23.6297)	β 0.2231 (0.0750)	δ 0.2097 (0.0697)	c 0.9255 (0.1433)	126.9844	132.9844	133.6145	138.8082	0.1770	1.1119	0.1949	0.1200	5.2608
OPGW-WP	α 0.9526 (0.3733)	β 0.3286 (0.0853)	λ 1.0884 (0.2268)	θ 1.3592×10^{-08} (0.0144)	108.8290	116.8290	118.0787	123.2724	0.0642	0.3950	0.1149	0.7130	0.0718

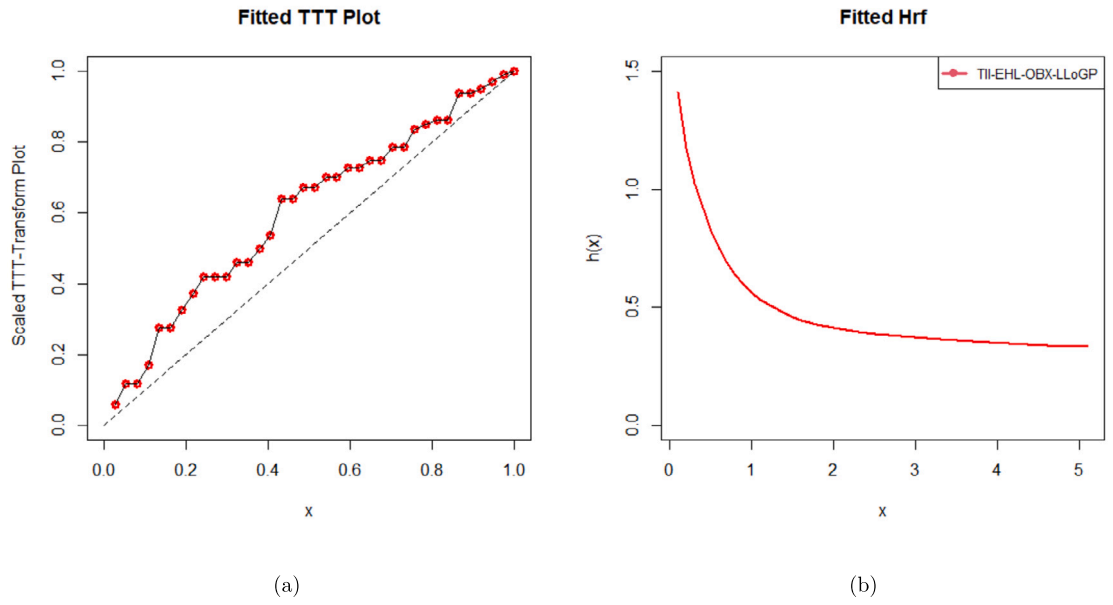

Fig. 14. Fitted (a) TTT and (b) Hrf Plots for Agriculture Data.

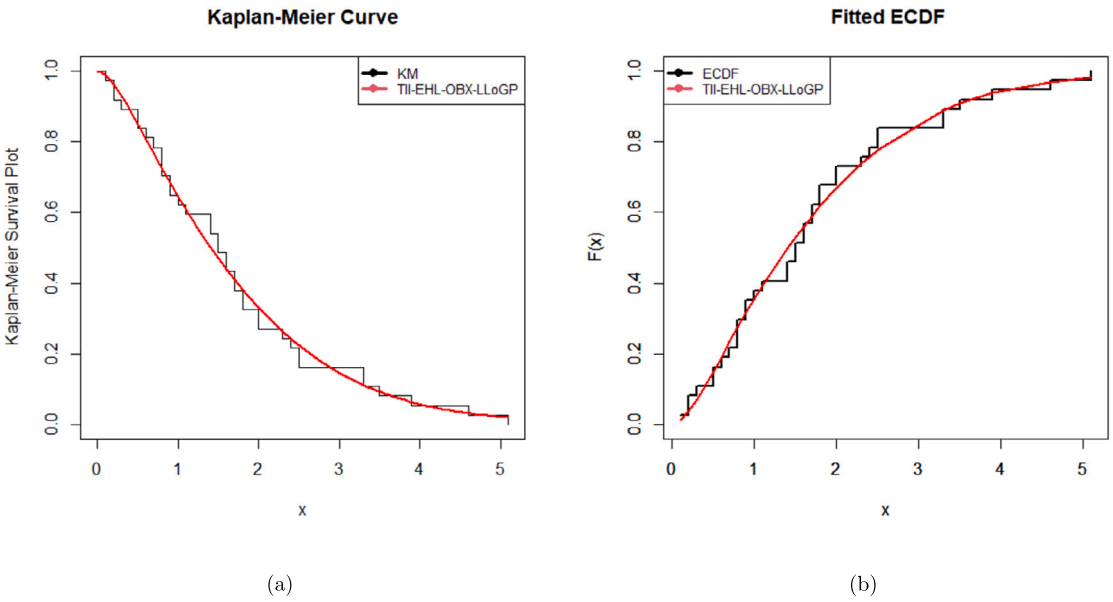

Fig. 15. Fitted (a) K-M and (b) EDCF Plots for Agriculture Data.

6.2. Survival years data

This data set represent survival years of patients who only received chemotherapy treatment and was applied by [6] and [36]. The data observation are given in appendix.

The estimated Var-Cov is

$$\begin{pmatrix} 0.0049 & -0.0252 & 0.0001 & -0.0001 \\ -0.0252 & 0.1293 & -0.0005 & 0.0006 \\ 0.0001 & -0.0005 & 2.0901\times10^{-06} & -2.5035\times10^{-06} \\ -0.0001 & 0.0006 & -2.5035\times10^{-06} & 2.2658\times10^{-05} \end{pmatrix}$$

and the estimated 95% CI for q, β, υ and c are respectively, given by 11.1940 ± 0.1369, 21.1730 ± 0.7049, 544.5300 ± 0.0028 and 0.0428 ± 0.0093, respectively.

Table 5
Estimates of Parameters and GoF Statistics for Survival Years Data.

	Estimates				Statistics								
Model	q	β	υ	c	$-2\log\hat{}$	AIC	$AICC$	BIC	CVM	AD	$K-S$	$P-VALUE$	SS
$TII-EHL-OBX-LLoGP(q,\beta,\upsilon,c)$	11.1940 (0.0702)	21.1730 (0.3593)	544.5300 (0.0014)	0.0428 (0.0047)	116.0108	124.0108	125.0108	131.2703	0.0746	0.5031	0.1062	0.6511	0.0759
$TII-EHL-OBX-LLoGP(1,\beta,\upsilon,c)$	- -	0.9989 (0.1383)	9.7509×10^{-09} (0.0198)	0.5000 (0.0499)	136.3235	142.3235	142.9088	147.7434	0.0650	0.4459	0.2712	0.0020	1.5798
$TII-EHL-OBX-LLoGP(1,1,\upsilon,c)$	- -	- -	2.8503×10^{-09} (0.0065)	0.4893 (0.0474)	136.2201	140.2201	140.5058	143.8334	0.0643	0.4417	0.2759	0.0016	14.9568
EBXIIP	c 0.9805 (1.0374)	s 0.0053 (1.3547×10^{-05})	α 1.0717 (1.1332)	λ 0.0059 (1.3223×10^{-05})	116.2498	124.2498	125.2498	131.4764	0.0811	0.5427	0.1082	0.6278	0.0799
GGP	θ 4.1348×10^{-08} (0.0390)	α 1.1611 (0.3498)	β 0.8064 (0.3526)	γ 3.2741×10^{-06} (0.2094)	116.2660	124.2660	125.2660	131.4926	0.0781	0.5246	0.1236	0.4602	0.1066
TLWP	α 0.4128 (0.4388)	β 0.9559 (0.5907)	λ 1.1789 (1.2740)	θ 1.9758×10^{-08} (0.0194)	116.2064	124.2064	125.2064	131.4330	0.0759	0.5113	0.1149	0.5532	14.9568
OEHLBXII	α 0.1287 (0.2843)	λ 0.0201 (0.2929)	a 6.2177 (12.1039)	b 0.5314 (0.5831)	118.1072	126.1072	127.1072	133.3338	0.0896	0.6010	0.1109	0.5973	0.0819
EHLOW-TL-LLoG	b 71.4475 (35.2931)	β 0.1926 (0.0790)	δ 0.1474 (0.1026)	c 0.8709 (0.1190)	129.4317	137.4317	138.4317	144.6588	0.0960	0.6739	0.1923	0.0622	7.2651
OPGW-WP	α 0.9363 (0.1444)	β 0.7269 (0.0856)	λ 0.3793 (0.0561)	θ 3.9246×10^{-09} (0.0079)	145.6448	153.6447	154.6447	160.8714	0.0730	0.4933	0.3013	0.0004	1.1348

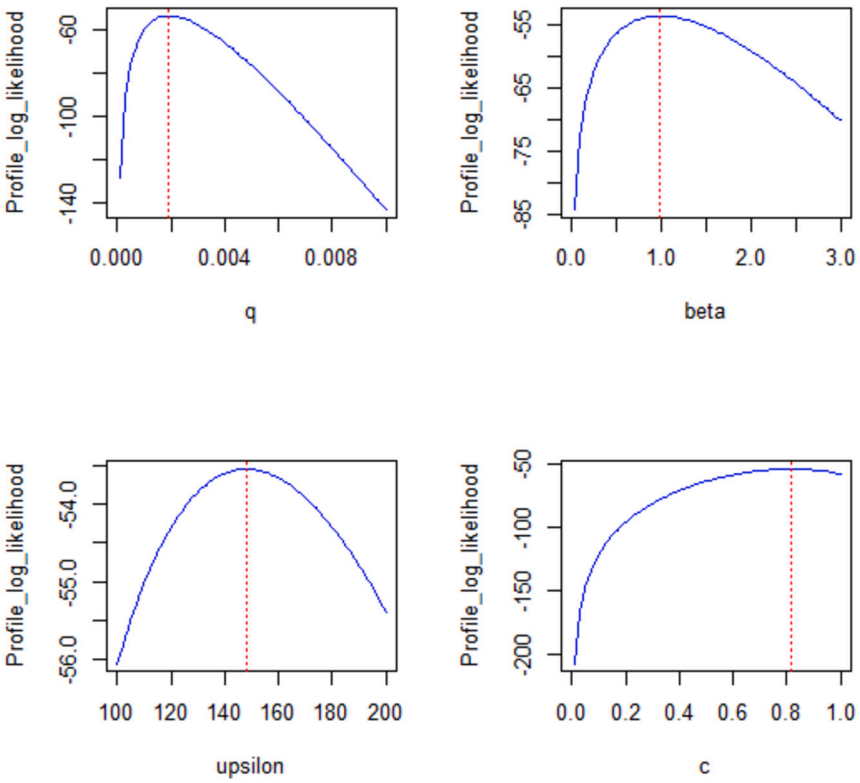

Fig. 16. Graphs of Profile Log-Likelihood Function of the Parameters of the TII-EHL-OBX-LLoGP Distribution on Agriculture Data.

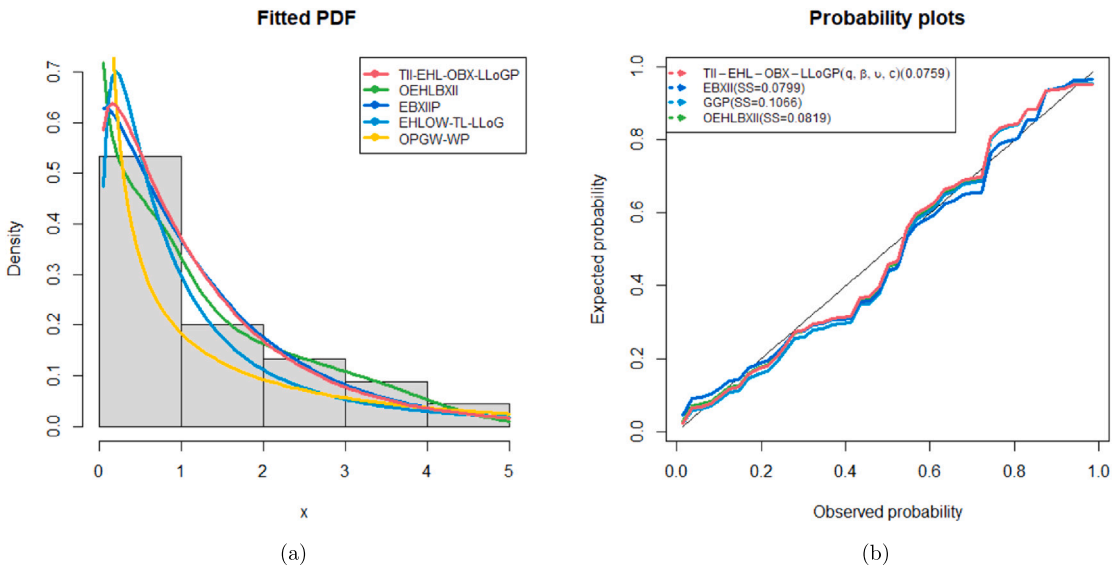

Fig. 17. Fitted (a) Pdf and (b) PP Plots for Survival Years Data.

As shown in Table 5, the TII-EHL-OBX-LLoGP distribution has lowest GoF statistics values and a highest p-value for the K-S statistic. The fitted pdf and PP plots for survival years data is shown in Fig. 17. These fitted plots supports the GoF statistics presented in Table 5 and further confirms that the TII-EHL-OBX-LLoGP distribution fits the survival years data in comparison to the models utilized for comparison in this study. Fig. 18 illustrates a TTT plot for survival years data, revealing an upside-down bathtub hrf. The K-M and ECDF curves for the survival years data are shown in Fig. 19. From the closeness of the empirical and fitted lines in Fig. 19, it can be inferred that TII-EHL-OBX-LLoGP model is a strong fit for the survival years data. Figs. 20 and 21 shows the

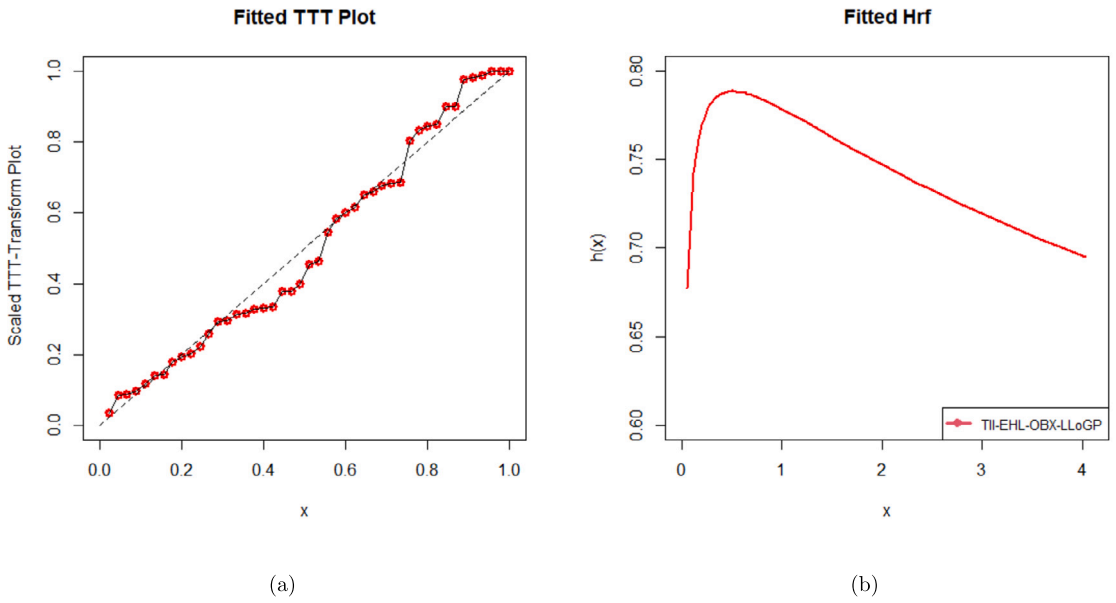

Fig. 18. Fitted (a) TTT and (b) Hrf Plots for Survival Years Data.

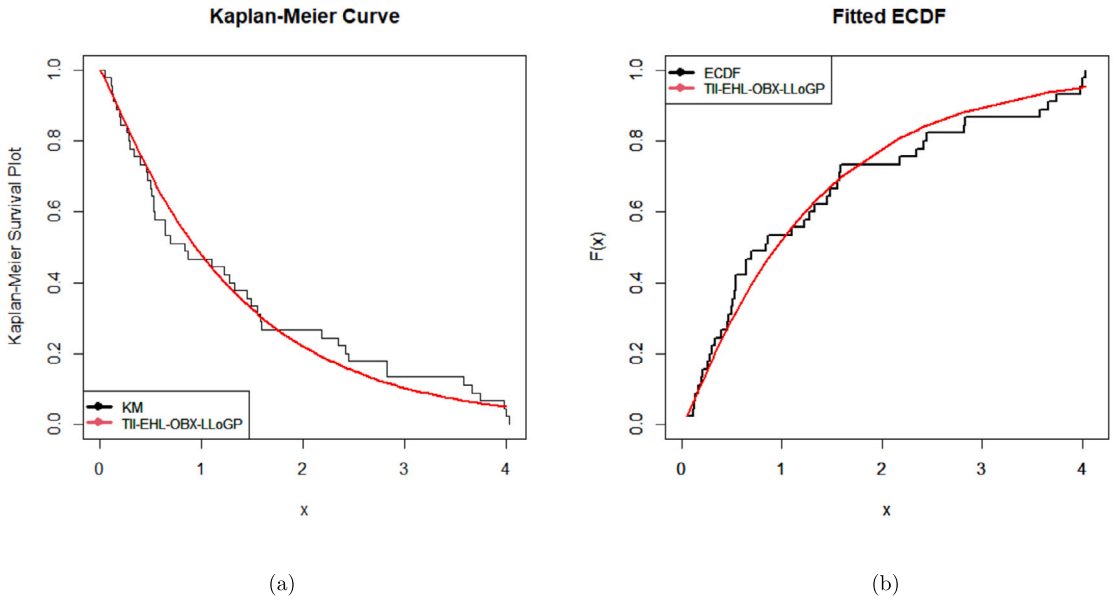

Fig. 19. Fitted (a) K-M and (b) ECDF Plots for Survival Years Data.

profile log-likelihood functions of TII-EHL-OBX-LLoGP distribution for survival years data. The MLEs for the TII-EHL-OBX-LLoGP distribution for the survival years exist and can be obtained uniquely, as illustrated in Figs. 20 and 21.

6.3. Carbon threads data

This data focuses on the fracture strength of carbon threads that measure a length of 50 mm. In the study [11], the data was put to use and is given in appendix.

The estimated Var-Cov matrix is

$$\begin{pmatrix} 6.6482\times10^{-05} & -0.0084 & 1.0224\times10^{-04} & -6.0914\times10^{-05} \\ -0.0084 & 1.0638 & -0.0129 & 0.0077 \\ 1.0224\times10^{-04} & -0.0129 & 1.5724\times10^{-04} & -9.3680\times10^{-05} \\ -6.0914\times10^{-05} & 0.0077 & -9.3681\times10^{-05} & 6.4380\times10^{-05} \end{pmatrix}$$

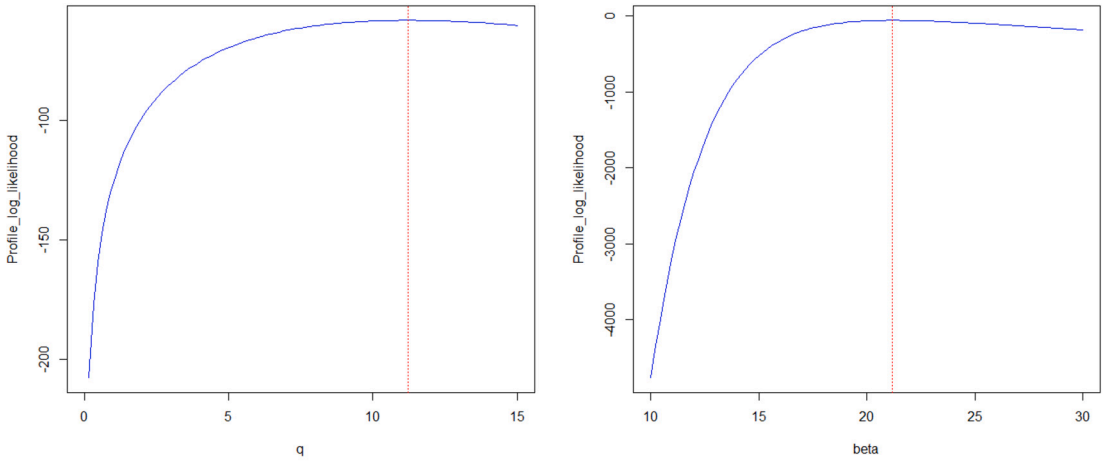

Fig. 20. Plots of the Profile Log-Likelihood Function of the Parameters (q and β) of the TII-EHL-OBX-LLoGP Distribution on Survival Years Data.

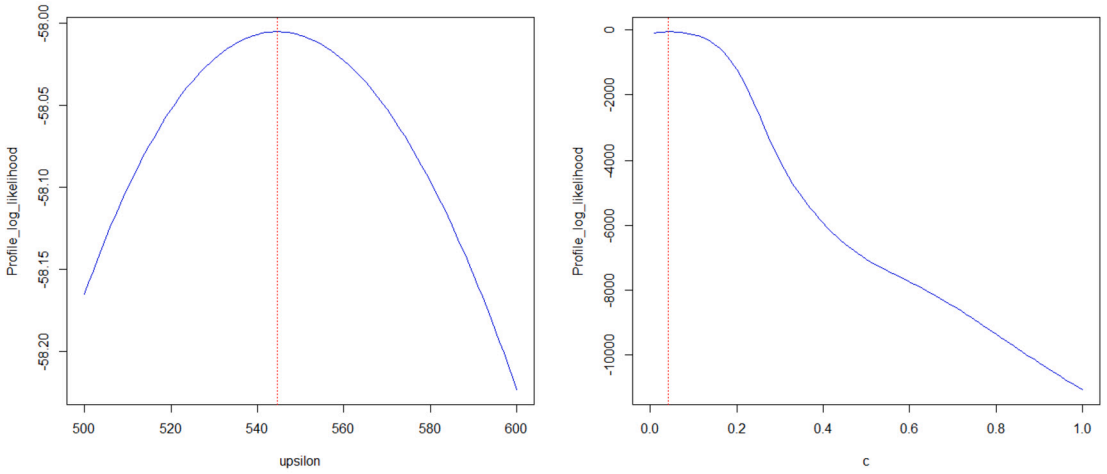

Fig. 21. Graphs of the Profile Log-Likelihood Functions of Parameters (υ and c) of the TII-EHL-OBX-LLoGP Distribution on Survival Years.

and the estimated 95% CI for q, β, υ and c can be respectively, expressed as follows: 270.7400 ± 0.0159, 33.8860 ± 2.0216, 174.2600 ± 0.0245 and 0.1000 ± 0.0157. The TII-EHL-OBX-LLoGP distribution has lowest GoF statistics and lowest K-S statistic with the largest p-value for the K-S statistics, as shown in Table 6. Fig. 22 confirms the GoF statistics in Table 6 with fitted pdf and PP for the carbon threads data set. The TII-EHL-OBX-LLoGP distribution exhibits a superior fit when contrasted with various other models. Fig. 23 represents the TTT plot for carbon threads data, illustrating an increasing hrf. The K-M survival and ECDF curves for carbon threads data set are shown in Fig. 24. Based on the closeness of the observed and fitted lines in Fig. 24, we conclude that TII-EHL-OBX-LLoGP fit the carbon threads data well. Figs. 25 and 26 presents the profile log-likelihood plots for the parameters of the TII-EHL-OBX-LLoGP distribution in the context of the carbon threads data. The MLEs for the TIIEHL-OBX-LLoGP distribution from carbon threads data are readily available and can be achieved uniquely, as shown in Figs. 25 and 26.

6.4. The Likelihood Ratio Test (LRT)

This section contains the LRT results for comparing the main model and nested distributions.

The performance of the nested models and the TII-EHL-OBX-LLoGP distribution differ significantly as shown by the results in Table 7. This demonstrates the importance of the additional parameters added to the parent distribution in improving model flexibility.

7. Conclusions

In this study, we presented the TII-EHL-OBX-GPS CoD, a versatile distribution developed to enhance the flexibility and adaptability of modeling real-world data. Our analysis encompassed a comprehensive examination of its mathematical characteristics, including qf, linear representation, raw moments, MGF, order statistics, and Rényi entropy. We demonstrated its ability to accommodate

Table 6
Estimates of Parameter and GoF Statistics for Carbon Threads Data.

	Estimates				Statistics								
Model	q	β	υ	c	$-2\log\ell$	AIC	$AICC$	BIC	CVM	AD	$K-S$	$P-VALUE$	SS
$TII-EHL-OBX-LLoGP(q,\beta,\upsilon,c)$	270.7400 (0.0081)	33.8860 (1.0314)	174.2600 (0.0125)	0.1000 (0.0080)	173.4101	181.4101	182.0658	190.1687	0.1124	0.6152	0.0883	0.6812	0.0947
$TII-EHL-OBX-LLoGP(1,\beta,\upsilon,c)$	- -	11.5770 (1.4213)	1.3597×10^{-05} (0.1146)	0.4638 (0.0268)	196.3670	202.3670	202.7541	208.9359	0.4399	2.4185	0.1645	0.0561	19.0606
$TII-EHL-OBX-LLoGP(1,1,\upsilon,c)$	- -	- -	1.9739×10^{-08} (0.1146)	0.3547 (0.0268)	420.2332	424.2332	424.4237	428.6125	0.2831	1.5464	0.7842	2.2000×10^{-16}	10.4748
EBXIIP	c 6.1732 (1.1258)	s 3.0602 (0.2167)	α 0.5338 (0.1449)	λ 2.1955×10^{-08} (0.0195)	175.8609	183.8609	184.5171	192.6200	0.1407	0.7515	0.1366	0.1698	0.2959
TLWP	α 0.0559 (0.0470)	β 2.3502 (0.5353)	λ 1.8256 (0.7757)	θ 1.4764×10^{-08} (0.0129)	175.1200	183.1200	183.7756	191.8785	0.1448	0.7731	0.1052	0.4573	0.1404
GGP	θ 4.7202 (1.6502	α 5.2044 (3.0043)	β 1.3099 (0.4256)	γ 1.6685×10^{-07} (0.1306)	178.8249	186.8249	187.4806	195.5835	0.2125	1.1199	0.1068	0.4386	0.1709
OEHLBXII	α 0.2969 (0.0786)	λ 0.0002 (0.0004)	a 7.7367 (0.0148)	b 0.8336 (0.1724)	194.4906	200.4906	203.1464	211.2493	0.1852	1.1959	0.1564	0.0791	0.2997
EHLOW-TL-LLoG	b 7.8607 (3.2976)	β 1.3858 (0.4371)	δ 1.05245 (0.4985)	c 0.9470 (0.2157)	174.7322	182.7322	183.3880	191.4909	0.1208	0.6758	0.1063	0.4441	0.1342
OPGW-WP	α 0.9213 (0.4312)	β 0.0480 (0.0237)	λ 2.3921 (0.2418)	θ 3.1060×10^{-07} (0.0505)	174.7643	182.7643	183.4200	191.5229	0.1193	0.7213	0.1137	0.3604	0.1374

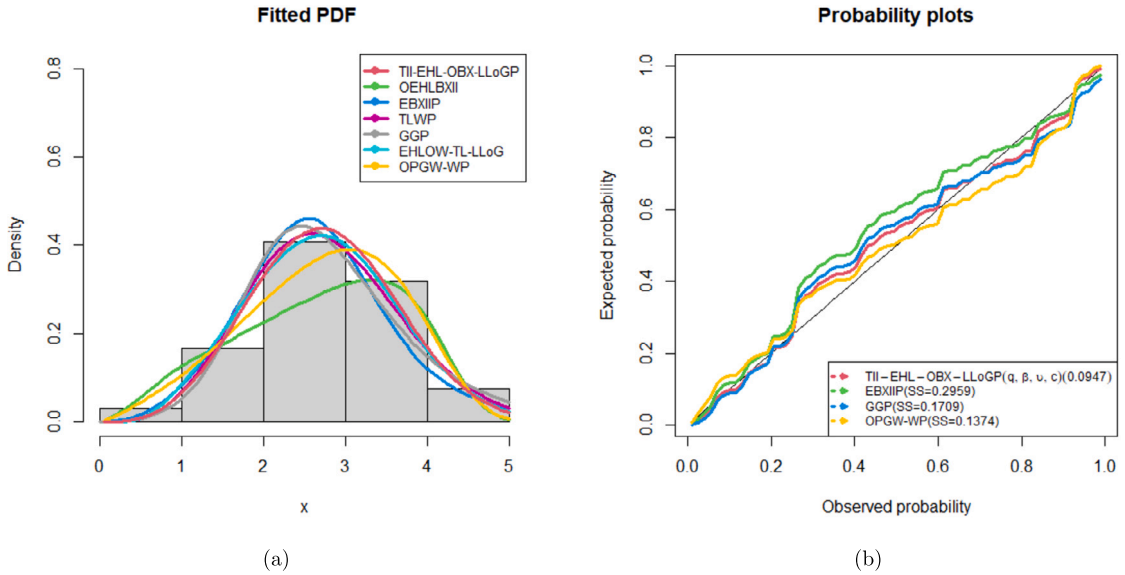

Fig. 22. Fitted (a) Pdf and (b) PP Plots for Carbon Threads Data.

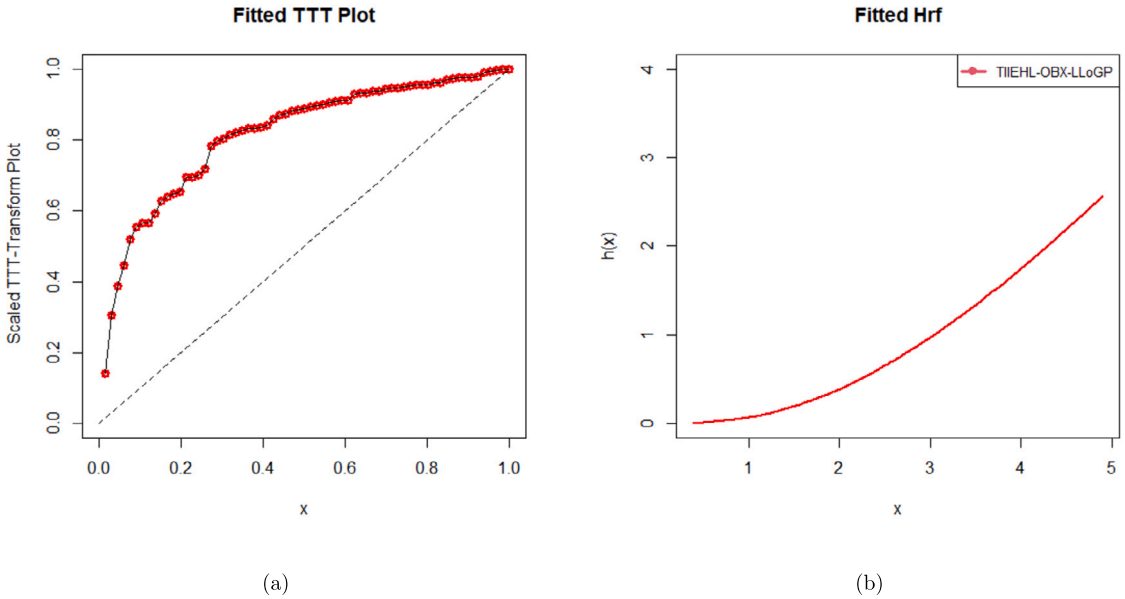

Fig. 23. Fitted (a) TTT and (b) Hrf Plots for Carbon Threads Data.

Table 7
LRT Results.

		Agriculture Data	Data from Patients Undergoing Chemotherapy	Carbon Threads Data
Nested Models	$degrees of freedom$	$\chi^2(p-value)$	$\chi^2(p-value)$	$\chi^2(p-value)$
TII-EHL-OBX-LLoGP(q, 1, υ, c)	1	8.9669(0.002749)	20.3127(0.000039)	22.9569(<0.00001)
TII-EHL-OBX-LLoGP(q, 1, 1, c)	2	50.7988(<0.00001)	20.2093(0.000041)	246.8231(<0.00001)

diverse data patterns, showcased the effectiveness of maximum likelihood estimation, and confirmed its consistent performance across various sample sizes through simulation studies. Practical applications highlighted the superiority of the TII-EHL-OBX-GPS CoD over nested and non-nested equi-parameter models. While this study has made significant contributions to the development of the TII-EHL-OBX-GPS CoD, there are several avenues for future research. Firstly, further investigations can explore the application of the TII-EHL-OBX-GPS CoD in dealing with diverse data types, such as censored datasets. Additionally, efforts can be made to

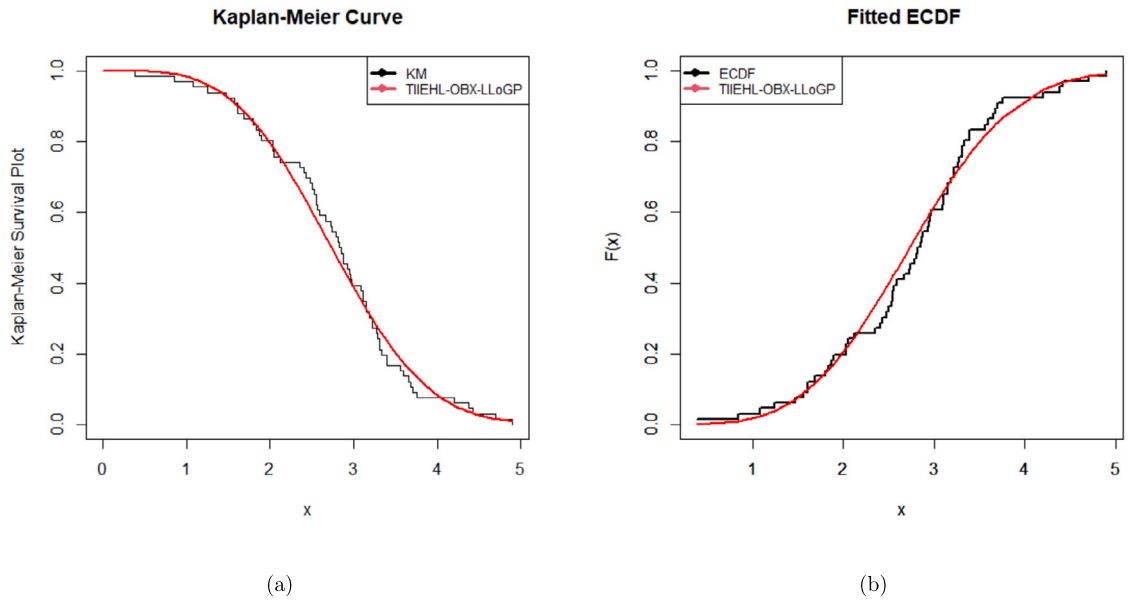

Fig. 24. Fitted (a) K-M and (b) EDCF Plots for Carbon Threads Data.

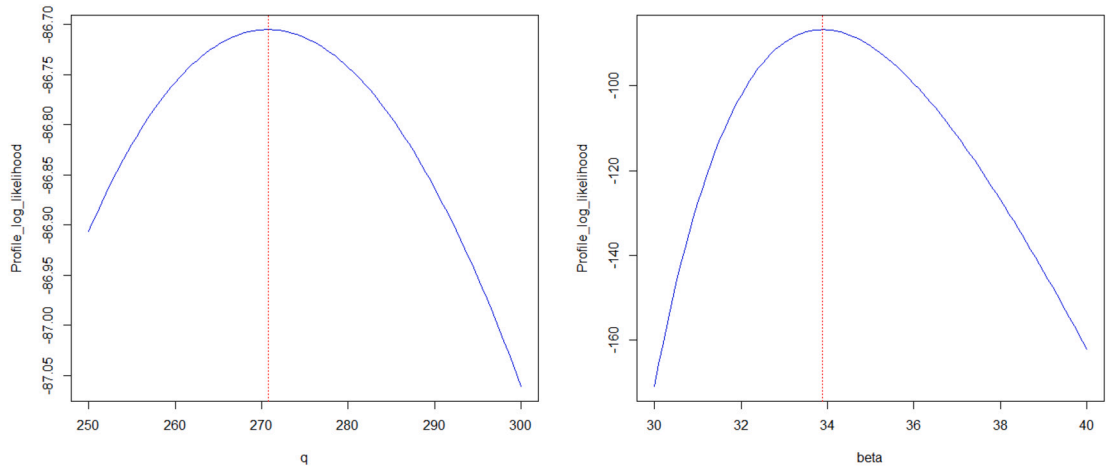

Fig. 25. Profile Log-Likelihood Functions Plots of the Parameters (q and β) of the TII-EHL-OBX-LLoGP Distribution on Carbon Threads Data.

use alternative parameter estimation methods. Also, bivariate extensions of TII-EHL-OBX-GPS CoD can be considered. These future research can improve the flexibility and applicability of the TII-EHL-OBX-GPS CoD, opening up new opportunities for advancements in data modeling and analysis.

CRediT authorship contribution statement

Neo Dingalo: Writing – review & editing, Writing – original draft. **Broderick Oluyede:** Writing – review & editing, Supervision, Conceptualization. **Fastel Chipepa:** Supervision, Writing – review & editing.

Declaration of competing interest

The authors declare the following financial interests/personal relationships which may be considered as potential competing interests: Neo Dingalo has patent pending to Licensee. Broderick Oluyede has patent pending to Licensee. Fastel Chipepa has patent pending to Licensee.

Data availability

Data included in article/supplementary material/referenced in article.

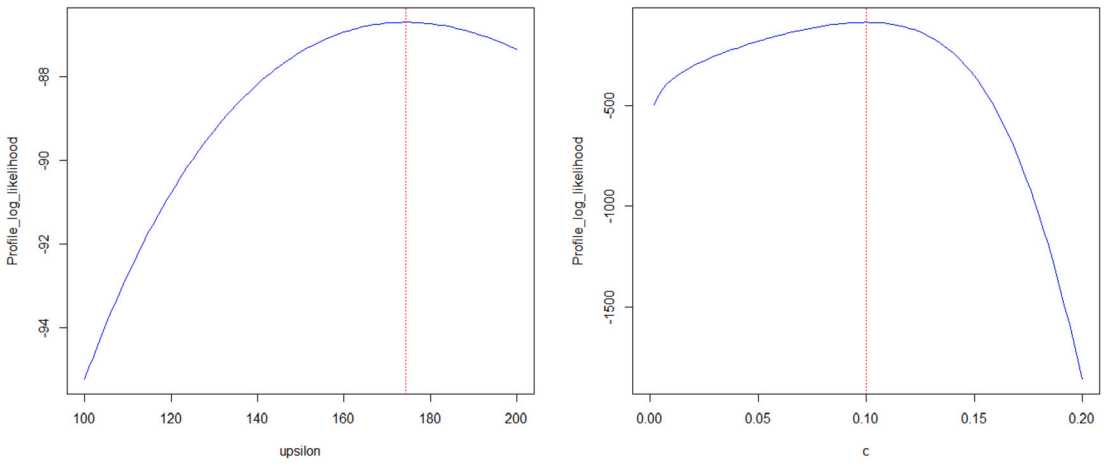

Fig. 26. Graphs of the Profile Log-Likelihood Function of the Parameters (υ and c) of TII-EHL-OBX-LLoGP Distribution on Carbon Threads Data.

Appendix A

The appendix materials are available at the URL below:
https://drive.google.com/file/d/1395qP7lhT8BggbNGStiit4ud4SpDTqXg/view?usp=share_link

References

[1] M.V. Aarset, How to identify bathtub Hazard rate, IEEE Trans. Reliab. 36 (1) (1987) 106–108.
[2] M.A.D. Aldahlan, A.Z. Afify, The odd exponentiated half-logistic Burr XII distribution, Pak. J. Stat. Oper. Res. 14 (2) (2018) 305–317.
[3] A. Algarni, A.M. Almarashi, I. Elbatal, A.S. Hassan, E.M. Almetwally, A.M. Daghistani, M. Elgarhy, Type I half logistic Burr X-G family: properties, Bayesian, and non-Bayesian estimation under censored samples and applications to COVID-19 data, Math. Probl. Eng. 2021 (2021) 1–21.
[4] H. Al-Mofleh, M. Elgarhy, A. Afify, M. Zannon, Type II exponentiated half logistic generated family of distributions with applications, Electron. J. Appl. Stat. Anal. 13 (2) (2020) 536–561.
[5] E. Altun, M. Alizadeh, H.M. Yousof, M. Rasekhi, G.G. Hamedani, A new type II half logistic-G family of distributions with properties, regression models, system reliability and applications, Appl. Appl. Math. 16 (2) (2021) 823–843, https://digitalcommons.pvamu.edu/aam/vol16/iss2/3.
[6] A. Bekker, J. Roux, P. Mostert, A generalization of the compound Rayleigh distribution: using a Bayesian methods on cancer survival times, Commun. Stat., Theory Methods 29 (7) (2000) 1419–1433.
[7] O.A. Bello, S.I. Doguwa, A. Yahaya, H.M. Jibril, A type II half logistic exponentiated-G family of distribution with applications to survival analysis, Fudma J. Sci. 5 (3) (2021) 177–190, https://doi.org/10.33003/fjs-2021-0503-717.
[8] F. Chipepa, B. Oluyede, B. Makubate, The new odd Lindley-G power series class of distributions: theory, properties and applications, Afr. Stat. 16 (3) (2021) 2825–2849.
[9] F. Chipepa, B. Oluyede, D. Wanduku, The exponentiated half logistic odd Weibull-Topp-Leone-G family of distributions: model, properties and applications, J. Stat. Model., Theory Appl. 2 (1) (2020) 15–38.
[10] F. Chipepa, B. Oluyede, D. Wanduku, T. Moakofi, The exponentiated half Logistic-Topp-Leone-G power series class of distributions: model, properties and applications, in: J. Singh, H. Dutta, D. Kumar, D. Baleanu, J. Hristov (Eds.), Methods of Mathematical Modelling and Computation for Complex Systems, in: Studies in Systems, Decision and Control, vol. 373, Springer, Cham, 2022, pp. 341–374.
[11] G.M. Cordeiro, A.J. Lemonte, The β-Birnbaum-Saunders distribution: an improved distribution for fatigue life modeling, Comput. Stat. Data Anal. 55 (3) (2011) 1445–1461.
[12] R.V. da Silva, F. Gomes-Silva, M.W.A. Ramos, G.M. Cordeiro, The exponentiated Burr XII Poisson distribution with applications to lifetime data, Int. J. Stat. Probab. 4 (4) (2015) 112–131.
[13] I. Elbatal, E. Altun, A.Z. Afify, G. Ozel, The generalized Burr XII power series distributions with properties and applications, Ann. Data Sci. 6 (3) (2019) 571–597.
[14] A.F. Fagbamigbe, P. Melamu, B.O. Oluyede, B. Makubate, The Ristić and Balakrishnan Lindley-Poisson distribution: model, theory and application, Afr. Stat. 13 (4) (2018) 837–1864.
[15] N.A. Ibrahim, M.A. Khaleel, F. Merovci, A. Kilicman, M. Shitan, Weibull-Burr X distribution properties and application, Pak. J. Stat. 33 (5) (2017) 315–336.
[16] F. Jamal, C. Chesneau, M. Elgarhy, Type II general inverse exponential family of distributions, J. Stat. Manag. Syst. 23 (3) (2020) 617–641.
[17] F. Jamal, M. Tahir, M. Alizadeh, M. Nasir, On Marshall-Olkin Burr X family of distribution, Tbil. Math. J. 10 (4) (2017) 175–199.
[18] M.G. Khalil, G.G. Hamedani, H.M. Yousof, The Burr X exponentiated Weibull model: characterizations, mathematical properties and applications to failure and survival times data, Pak. J. Stat. Oper. Res. 15 (1) (2019) 141–160.
[19] U.Y. Madaki, M.R.A. Bakar, L. Handique, Beta Kumaraswamy Burr type X distribution and its properties, Preprints 1 (2018) 2018080304, https://doi.org/10.20944/preprints201808.0304.v1.
[20] B. Makubate, M. Gabanakgosi, F. Chipepa, B. Oluyede, A new Lindley-Burr XII power series distribution: model, properties, and applications, Heliyon 7 (6) (2021) e07146.
[21] B. Makubate, K. Rannona, B. Oluyede, F. Chipepa, The Topp-Leone-G power series class of distributions with applications, Pak. J. Stat. Oper. Res. 17 (4) (2021) 827–846, https://doi.org/10.18187/pjsor.v17i4.3636.
[22] F. Merovci, M.A. Khaleel, N.A. Ibrahim, M. Shitan, The Beta Burr type X distribution properties with application, SpringerPlus 5 (1) (2016) 1–18.
[23] T. Moakofi, B. Oluyede, Type II exponentiated half-logistic Gompertz-G family of distributions: properties and applications, Math. Slovaca 73 (3) (2023) 785–810.
[24] T. Moakofi, B. Oluyede, F. Chipepa, Type II exponentiated Half-Logistic-Topp-Leone-G power series class of distributions with applications, Pak. J. Stat. Oper. Res. 17 (4) (2021) 885–909.
[25] T. Moakofi, B. Oluyede, F. Chipepa, Type II exponentiated half-logistic Topp-Leone Marshall-Olkin-G family of distributions with applications, Heliyon 7 (12) (2021) e08590.

[26] B. Oluyede, F. Chipepa, D. Wanduku, The odd Weibull–Topp–Leone–G power series family of distributions: model, properties and applications, J. Nonlinear Sci. Appl. 14 (4) (2021) 268–286.
[27] B. Oluyede, F. Chipepa, D. Wanduku, Exponentiated half logistic-power generalized Weibull-G family of distributions: model, properties and applications, Euras. Bull. Math. 3 (3) (2021) 134–161.
[28] B.O. Oluyede, B. Makubate, A.F. Fagbamigbe, P. Mdlongwa, A new Burr XII-Weibull-Logarithmic distribution for survival and lifetime data analysis: model, theory, and applications, Stats 1 (1) (2018) 77–91.
[29] B.O. Oluyede, B. Mashabe, A. Fagbamigbe, B. Makubate, D. Wanduku, The exponentiated generalized power series: family of distributions: theory, properties and applications, Heliyon 6 (8) (2020) e04653.
[30] B. Oluyede, T. Moakofi, Type II exponentiated half-logistic-Gompertz Topp-Leone-G family of distributions with applications, Central Eur. J. Econ. Model. Econometr. 14 (4) (2022) 225–262.
[31] B. Oluyede, T. Moakofi, F. Chipepa, The odd power generalized Weibull-G power series class of distributions: properties and applications, Stat. Trans. New Ser. 23 (1) (2022) 89–108.
[32] P. Osatohanmwen, F.O. Oyegue, S.M. Ogbonmwan, The T–R Y power series family of probability distributions, J. Egypt. Math. Soc. 28 (1) (2020) 1–18.
[33] M. Pararai, G. Warahena-Liyanage, B.O. Oluyede, Exponentiated power Lindley–Poisson distribution: properties and applications, Commun. Stat., Theory Methods 46 (10) (2017) 4726–4755.
[34] A. Rényi, On measures of entropy and information, in: Proceedings of the Fourth Berkeley Symposium on Mathematical Statistics and Probability, vol. 4(1), 1960, pp. 547–561.
[35] M.K. Shakhatreh, S. Dey, D. Kumar, Inverse Lindley power series distributions: a new compounding family and regression model with censored data, J. Appl. Stat. 49 (13) (2021) 3451–3476, https://doi.org/10.1080/02664763.2021.1951683.
[36] D.M. Stanblen, W.H. Carter, J.W. Novak, Analysis of survival data with non-proportional Hazard functions, Control. Clin. Trials 2 (2) (1981) 149–159.
[37] A.H. Soliman, M.A.E. Elgarhy, M. Shakil, Type II half logistic family of distributions with applications, Pak. J. Stat. Oper. Res. 13 (2) (2017) 245–264.
[38] S. Tahmasebi, A.A. Jafari, Exponentiated extended Weibull-power series class of distributions, Cienc. Nat., Santa Maria 37 (2) (2015) 183–193.
[39] S. Tahmasebi, A.A. Jafari, Generalized Gompertz-power series distributions, in: Hacettepe, J. Math. Stat. 45 (5) (2015) 1579–1604.